ORIGINAL RESEARCH

m^{6}A-Methylated NUTM2B-AS1 Promotes Hepatocellular Carcinoma Stemness Feature via Epigenetically Activating *BMPR1A* Transcription

Wenchuan Li[1,2,]*, Min Zeng[3,]*, Yuanjia Ning[3,]*, Rongzhou Lu[3], Yunyu Wei[3], Zuoming Xu[2], Huamei Wei[1,4], Jian Pu[1,2]

[1]Guangxi Clinical Medical Research Center for Hepatobiliary Diseases, Baise, People's Republic of China; [2]Department of Hepatobiliary Surgery, Affiliated Hospital of Youjiang Medical University for Nationalities, Baise, People's Republic of China; [3]Graduate College of Youjiang Medical University for Nationalities, Baise, People's Republic of China; [4]Department of Pathology, Affiliated Hospital of Youjiang Medical University for Nationalities, Baise, People's Republic of China

*These authors contributed equally to this work

Correspondence: Jian Pu, Guangxi Clinical Medical Research Center for Hepatobiliary Diseases, No. 18 Zhongshan Two Road, Baise, 533000, People's Republic of China, Email jian_pu@126.com

Purpose: Hepatocellular carcinoma (HCC) is one of the most lethal malignancies in the world. Oncofetal proteins are the optimal diagnostic biomarkers and therapeutic targets for HCC. As the most abundant modification in RNA, N^6-methyladenosine (m^{6}A) has been reported to be involved in HCC initiation and progression. However, whether m^{6}A has oncofetal characteristics remains unknown.

Methods: Gene expression in HCC tissues and cells was detected using qPCR. The level of m^{6}A methylation was determined using methylated RNA immunoprecipitation assay. The biological roles of NUTM2B-AS1 in HCC were detected using Cell Counting Kit-8, 5-ethynyl-2'-deoxyuridine incorporation, and spheroid formation assays. The mechanisms underlying the roles of NUTM2B-AS1 were explored using RNA immunoprecipitation (RIP), chromatin isolation by RNA purification (ChIRP), chromatin immunoprecipitation (ChIP), and assay for transposase-accessible chromatin (ATAC).

Results: NUTM2B-AS1 was identified as a novel oncofetal long noncoding RNA that was upregulated in the fetal liver and HCC and silenced in adult liver tissues. METTL3 and METTL16 induce m^{6}A hypermethylation of NUTM2B-AS1. The m^{6}A methylation levels of NUTM2B-AS1 exhibit oncofetal characteristics. m^{6}A methylation upregulates NUTM2B-AS1 expression by increasing NUTM2B-AS1 transcript stability. m^{6}A-methylated NUTM2B-AS1 promotes HCC cell proliferation and stemness via epigenetically activating *BMPR1A* expression. NUTM2B-AS1 specifically binds to *BMPR1A* promoter. m^{6}A-methylated NUTM2B-AS1 is recognized by the m^{6}A reader YTHDC2, which further binds to the H3K4 methyltransferase MLL1. m^{6}A-methylated NUTM2B-AS1 recruits YTHDC2 and MLL1 to *BMPR1A* promoter, leading to increased H3K4me3 and chromatin accessibility at *BMPR1A* promoter. Functional rescue assays suggest that BMPR1A is a critical mediator of the oncogenic role of m^{6}A-methylated NUTM2B-AS1 in HCC.

Conclusion: METTL3- and METTL16-mediated m^{6}A methylation of NUTM2B-AS1 is a novel oncofetal molecular event in HCC that promotes HCC stemness via epigenetically activating *BMPR1A* transcription.

Keywords: N^6-methyladenosine, oncofetal molecule, hepatocellular carcinoma, stemness, histone modification

Introduction

Liver cancer is one of the most common malignancies worldwide, which ranks as the second leading lethal cancer type in China and the sixth leading lethal cancer type in the United States.[1,2] Hepatocellular carcinoma (HCC) is the major subtype of liver cancer.[3] Compared to other malignancies, HCC has relatively poor prognosis, with 5-year survival rate of only about 20%.[4] One of the causes of worse prognosis of HCC is that most HCCs have stemness property and strong

self-renewal potential.[5] HCC share many similar molecular features with embryonic liver development.[6] Several oncofetal molecules have been identified in HCC, such as AFP, GPC3, SALL4, MBNL3, H19 and SLC38A4.[7–12] However, other oncofetal events, such as epigenetic modifications, involved in embryonic liver development and HCC are still largely unknown.

Epigenetic modifications are the main regulators of gene expression and include DNA methylation, histone modification, and noncoding RNAs etc.[13–15] Long noncoding RNAs (lncRNAs) are a class of regulatory noncoding RNAs that are more than 200 nucleotides in length and have no protein encoding potential.[16–18] Many reports have revealed the critical roles of lncRNAs in various diseases, including HCC.[19–21] lncRNA PVT1 and MIR4435-2HG were previously identified as oncofetal lncRNAs in HCC.[22,23] However, whether other lncRNAs could also be recognized as oncofetal events and their potential roles in HCC need further investigation.

As the most abundant modification in RNA, N^6-methyladenosine (m^{6}A) is another level of epitranscriptomic regulation of gene expression.[24–26] Accumulating evidence has shown that m^{6}A methylation can occur in both coding and noncoding transcripts, which plays important roles in modulating the fate of modified transcripts, including processing, stability, translation etc.[27–29] m^{6}A methylation is catalyzed by m^{6}A methyltransferases, such as METTL3, METTL14, METTL16, and WTAP.[30–32] Some transcripts may be the common targets of various methyltransferases. In contrast to METTL3, METTL16 only methylates a limited number of targets.[33] m^{6}A methylation is a reversible modification, which can be removed by m^{6}A demethylases, such as FTO, ALKBH5, and ALKBH3.[34,35] The biological roles of m^{6}A are largely mediated by m^{6}A readers, such as YTHDC1, YTHDC2, YTHDF1, HNRNPA2B1 etc.[29,36] These m^{6}A readers recognize m^{6}A methylation and further bind other proteins to change the fate of m^{6}A-methylated transcripts.[37–39] Oncofetal m^{6}A methylation events in HCC are still largely unknown.

In this study, using a combinational analysis of lncRNAs dysregulated in fetal livers derived from GSE225635 data and lncRNAs dysregulated in HCC derived from The Cancer Genome Atlas (TCGA) Liver Hepatocellular Carcinoma (LIHC) data, we identified NUTM2B-AS1 as an oncofetal lncRNA. Furthermore, we found that m^{6}A methylation of NUTM2B-AS1 was also an oncofetal event. Functional investigations revealed that only m^{6}A-methylated NUTM2B-AS1 promoted HCC cell proliferation and enhanced the stemness features. Mechanistic investigations revealed that m^{6}A-methylated NUTM2B-AS1 epigenetically activated *BMPR1A* expression, which mediated the oncogenic role of m^{6}A-methylated NUTM2B-AS1 in HCC. BMPR1A belongs to the bone morphogenetic protein (BMP) receptor family, which drives HCC stem cell self-renewal through BMP signaling.[40–42]

Materials and Methods
Human Tissue Samples
Sixty pairs of HCC tissues and matched non-cancerous liver tissues were collected from patients with HCC who underwent surgery at the Affiliated Hospital of Youjiang Medical University for Nationalities. Fetal liver tissues were collected from patients who underwent pregnancy termination at the Affiliated Hospital of Youjiang Medical University for Nationalities. Adult liver tissues were collected from healthy distal liver tissues obtained from patients with liver hemangiomas at the Affiliated Hospital of Youjiang Medical University for Nationalities. Written informed consent was obtained from all the patients. This study was conducted in accordance with the Declaration of Helsinki and was reviewed and approved by the Affiliated Hospital of Youjiang Medical University for Nationalities Institutional Review Board.

Data Collection
The RNA-sequence data and clinical characteristics of 371 hCC patients derived from TCGA LIHC data were downloaded and analyzed using the online bioinformatics tools GEPIA (http://gepia.cancer-pku.cn/) and R2 Genomics Analysis and Visualization Platform (https://hgserver1.amc.nl/cgi-bin/r2/main.cgi). The lncRNA microarray data of 3 adult livers and 3 fetal livers was downloaded from GEO (https://www.ncbi.nlm.nih.gov/geo/) with the accession number GSE225635.[23]

Cell Culture

The human immortalized liver cell line THLE-2 (cat. no. CRL-2706), and HCC cell line SNU-398 (cat. no. CRL-2233) were obtained from American Type Culture Collection (ATCC, Manassas, VA, USA). The human HCC cell line, Hep3B (cat. no. SCSP-5045) and HuH-7 (cat. no. SCSP-526) cells were acquired from the Chinese Academy of Sciences Cell Bank (Shanghai, China). THLE-2 cells were cultured using the BEGM Bullet Kit (cat. no. CC-3170; Lonza, Basel, Switzerland). SNU-398, Hep3B, and HuH-7 cells were maintained in RPMI 1640 medium (Invitrogen, Carlsbad, CA, USA), Eagle's Minimum Essential Medium (Invitrogen), and Dulbecco's modified Eagle's medium (Invitrogen), respectively, supplemented with 10% fetal bovine serum (Invitrogen). All cells were cultured at 37°C in an atmosphere containing 5% CO_2 and were routinely tested as mycoplasma-free.

RNA Extraction, Reverse Transcription and Quantitative Polymerase Chain Reaction (qPCR)

Total RNA was isolated from the indicated tissues and cells using the RNA isolater Total RNA Extraction Reagent (cat. no. R401, Vazyme, Nanjing, China). Reverse transcription was performed using the HiScript III RT SuperMix for qPCR (cat. no. R323, Vazyme). qPCR was conducted using the ChamQ Universal SYBR qPCR Master Mix (cat. no. Q711, Vazyme) and gene-specific primers. The sequences of primers were as follows: 5'-TCAACCATCTTTCCTGTGA-3' (sense) and 5'-TCTGAAA AGTGTCTTGTCTGT-3' (antisense) for NUTM2B-AS1, 5'-GGTATGAACGGGTAGATGA-3' (sense) and 5'-GTTGAA GCCTTGGGGATT-3' (antisense) for METTL3, 5'-GGTCGGACAATGAGATGG-3' (sense) and 5'-GGTGATGCTTTGAG GGATA-3' (antisense) for METTL16, 5'-TGCTGGCACTGCTCCTAC-3' (sense) and 5'-AAGAGACTGGCTGTTGACT-3' (antisense) for CD24, 5'-ATGGACAAGTTTTGGTGG-3' (sense) and 5'-TGTGGGCAAGGTGCTATT-3' (antisense) for CD44, 5'-GGACTTGCGAACTCTCTTG-3' (sense) and 5'-CCTCTTTGGTCTCCTTGAT-3' (antisense) for CD133, 5'-AAA CAGGAAGGGATGGAA-3' (sense) and Please indicate where it should be pl5'-CAGATGACGAAGAGCACAG-3' (antisense) for CTNNB1, 5'-AGGTGAATCCTTGTTTCAT-3' (sense) and 5'-TCTCAGCCTTCTCATACTTT-3' (antisense) for EPCAM, 5'-GCCTTTGTGCTTCTGTTCTTCG-3' (sense) and 5'-CCCACTCATTCTGGTTGTCGTC-3' (antisense) for NOTCH1, 5'-GAGATGGCTCGTCGTTGT-3' (sense) and 5'-TCTGGAGGCTGGATTGTG-3' (antisense) for BMPR1A, 5'-GTCGGAGTCAACGGATTTG-3' (sense) and 5'-TGGGTGGAATCATATTGGAA-3' (antisense) for GAPDH. GAPDH was used as an endogenous control. Relative expression was calculated using the $2^{-\Delta\Delta Ct}$ method.

Vectors Construction, Cell Transfection and Stable Cell Line Construction

NUTM2B-AS1 full-length sequence was PCR-amplified using PrimeSTAR Max DNA Polymerase (cat. no. R045Q; Takara, Shiga, Japan) and primers 5'-AACTTAAGCTTGGTACCGGCCCTCCGGCTGAGCC-3' (sense) and 5'-TTTAAACGGGCCCTCTAGAACTTTAAAAAATATTAACATTTACT-3' (antisense). The PCR product was cloned into the *Kpn* I and *Xba* I sites of pcDNA3.1$^{(+)}$ vector (cat. no. V79020; Invitrogen), using a NovoRec plus one-step PCR Cloning Kit (cat. no. NR005; Novoprotein, Shanghai, China) to construct a NUTM2B-AS1 expression vector. m^{6}A-modification sites (70, 130, 568, 679, and 810) mutated NUTM2B-AS1 expression vectors were constructed using the Fast Mutagenesis System (cat. no. FM111, TransGen, Beijing, China) and the primers 5'-TGTGGTCCACCGGAGGTCTCCCTACATTC-3' (sense) and 5'-ACCTCCGGTGGACCACACTCCTTCTAGC-3' (antisense) for mutation of the 70th site, 5'-CTGGGAT ACCGGAGGTCTCGGGTCCC-3' (sense) and 5'-ACCTCCGGTATCCCAGCAGCCACCGG-3' (antisense) for mutation of the 130th site, 5'-GTTCTGATACTAAGGTCAAGTATCAACC-3' (sense) and 5'-ACCTTAGTATCAGAACAATCTCC AGTG-3' (antisense) for mutation of the 568th site, 5'-CATATGACATTAACAGTCAAGACACTTTTC-3' (sense) and 5'-ACTGTTAATGTCATATGAGCCCCTGTG-3' (antisense) for mutation of the 679th site, 5'-AAATGTTA TATTTGGGTCTGTTATCTAAT-3' (sense) and 5'-ACCCAAATATAACATTTAACTGTACATC-3' (antisense) for mutation of the 810th site. The NUTM2B-AS1 expression vector and m^{6}A-modification site-mutated NUTM2B-AS1 expression vectors were transfected into SNU-398 and Hep3B cells using GP-transfect-Mate (cat. no. G04009, GenePharma, Shanghai, China). Transfected cells were treated with 800 µg/ml of G418 (cat. no. ant-gn-1, InvivoGen, San Diego, CA, USA) for four weeks to select wild-type or m^{6}A methylation sites mutated NUTM2B-AS1 stably overexpressed HCC cells.

Two pairs of cDNA oligonucleotides targeting NUTM2B-AS1 were synthesized and subcloned into the shRNA lentivirus-expressing vector LV-3 (cat. no. C06003; GenePharma), which was used to generate shRNA lentiviruses targeting NUTM2B-AS1. A scrambled non-targeting shRNA lentivirus was used as the negative control (NC). The sequences of shRNA oligonucleotides were as follows: 5'-GATCCGGACAAGTATCAACCATCTTTTTCAAGAGAAAAGATGGTTGATACTTGTCCTTTTTTG-3' (sense) and 5'-AATTCAAAAAAGGACAAGTATCAACCATCTTTTCTCTTGAAAAAGATGGTTGATACTTGTCCG-3' (antisense) for shRNA-NUTM2B-AS1-1, 5'-GATCCGGCCACATCTAAGAAATCTTTTTCAAGAGAAAAGATTTCTTAGATGTGGCCTTTTTTG-3' (sense) and 5'-AATTCAAAAAAGGCCACATCTAAGAAATCTTTTCTCTTGAAAAAGATTTCTTAGATGTGGCCG-3' (antisense) for shRNA-NUTM2B-AS1-2, 5'-GATCCGTTCTCCGAACGTGTCACGTTTCAAGAGAACGTGACACGTTCGGAGAACTTTTTTG-3' (sense) and 5'-AATTCAAAAAAGTTCTCCGAACGTGTCACGTTCTCTTGAAACGTGACACGTTCGGAGAACG-3' (antisense) for shRNA-NC. HuH-7 cells were infected with shRNA lentiviruses targeting NUTM2B-AS1 and treated with 2 μg/ml puromycin (cat. no. ant-pr-1, InvivoGen) for four weeks to select NUTM2B-AS1 stably depleted HuH-7 cells.

METTL3 and METTL16 expression vectors were purchased from GenePharma. ON-TARGETplus Human METTL3 siRNA SMART Pool (Cat. no. L-005170-02-0010), ON-TARGETplus Human METTL16 siRNA SMART Pool (Cat. no. L-016359-02-0010), ON-TARGETplus Human YTHDC2 siRNA SMART Pool (Cat. no. L-014220-01-0010), ON-TARGETplus Human MLL1 siRNA SMART Pool (Cat. no. L-009914-00-0010) and ON-TARGETplus Human BMPR1A siRNA SMART Pool (cat. no. L-004933-00-0010) were purchased from Horizon Discovery (Cambridge, UK). Cell transfection was performed using GP-transfect-Mate (cat. no. G04009, GenePharma).

Cell Proliferation Assays

Cell Counting Kit-8 (CCK-8) and 5-ethynyl-2'-deoxyuridine (EdU) assays were conducted to evaluate cell proliferation, as previously described.[43–45] For the CCK-8 assay, 2000/well indicated cells were seeded into 96-well plates. After culturing for the indicated time, CCK-8 reagent (cat. no. CK04; Dojindo, Shanghai, China) was added to each well to measure the cell proliferation. The EdU assay was conducted using the Cell-Light EdU Apollo567 In Vitro Kit (cat. no. C10310-1, RiboBio, Guangzhou, China).

Flow Cytometry

Flow cytometry was conducted on the Attune NxT Flow Cytometer with Attune NxT Software version 5.2 (Thermo Fisher Scientific, Waltham, Massachusetts, USA) to detect samples using PE anti-human CD24 Antibody (cat. no. 311106, BioLegend, San Diego, CA, USA) or APC anti-human CD133 Antibody (cat. no. 397906, BioLegend). The data was analyzed by FlowJo version 10.8.0.

Spheroids Formation Assay

A total of 1000 cells were plated in each well of 6-well ultra-low attachment culture dishes with 2 ml culture medium and incubated for 10 days. The spheroids were photographed and counted using an inverted microscope.

Limiting Dilution Assay

SNU-398 cells were dissociated into single cells, serially diluted to the indicated doses, and mixed with matrigel at a ratio of 1:1. Then, the mixtures were injected into the flanks of 6-week old nude mice. After four weeks, the number of tumors was counted. This study was carried out following the specific animal treatment guidelines and was approved by the Affiliated Hospital of Youjiang Medical University for Nationalities Institutional Review Board.

RNA Immunoprecipitation (RIP) and Methylated RNA Immunoprecipitation (MeRIP) Assays

The binding of RNA to proteins was detected using the RIP assay, which was conducted in SNU-398 cells using an EZ-Magna RIP Kit (cat. no. 17–701, Millipore, Billerica, MA, USA) and antibodies against YTHDC2 (cat. no. ab220160, Abcam, Cambridge, MA, USA) or MLL1 (cat. no. 34907; Cell Signaling Technology, Danvers, MA). Enriched

NUTM2B-AS1 was measured using qPCR, as described above. The m^{6}A methylation level of NUTM2B-AS1 in HCC tissues and cells was measured using a MeRIP assay with a Magna MeRIP m^{6}A Kit (cat. no. 17–10499, Millipore). Enriched m^{6}A-methylated NUTM2B-AS1 was measured by qPCR, as described above.

Chromatin Isolation by RNA Purification (ChIRP) Assay

The binding of RNA to chromatin DNA was detected using the ChIRP assay, which was conducted in SNU-398 cells using the EZ-Magna ChIRP RNA Interactome Kit (cat. no. 17–10495, Millipore) and NUTM2B-AS1 antisense probes. The sequences of NUTM2B-AS1 antisense probes were as follows: 1, 5'-cgcggaaaccatagagatca-3'; 2, 5'-gaggc agtgaggtaatggag-3'; 3, 5'-agaactagaggtattccccg-3'; 4, 5'-tcttgcttcatggagccatg-3'; 5, 5'-atggttttgcttttatcctg-3'; 6, 5'-caccag taaagcttctcttc-3'; 7, 5'-agatggttgatacttgtcct-3'; 8, 5'-tgttaatgtcatatgagccc-3'. Enriched DNA was measured by qPCR using primers 5'-TGTGGGGCTGGCTTGTGG-3' (sense) and 5'-CCCGAAGAGTTCGCGGAG-3' (antisense) for *BMPR1A* promoter and 5'-GGCTACTAGCGGTTTTACGG-3' (sense) and 5'-CGAACAGGAGGAGCAGAGA-3' (antisense) for *GAPDH* promoter.

Chromatin Immunoprecipitation (ChIP) Assay

Histone modification levels in the indicated HCC cells were detected using the ChIP assay, which was conducted using an EZ-Magna ChIP A/G Kit (cat. no. 17–10086, Millipore) and antibodies against H3K9me2 (cat. no. ab1220; Abcam) or H3K4me3 (cat. no. ab8580, Abcam). Binding of proteins to chromatin DNA was also detected using the ChIP assay, which was conducted in HCC cells using the EZ-Magna ChIP A/G Kit (cat. no. 17–10086, Millipore) and antibodies against YTHDC2 (cat. no. ab220160; Abcam) or MLL1 (cat. no. 34907; Cell Signaling Technology). The enriched *BMPR1A* promoter region was measured by qPCR using the primers 5'-TGTGGGGCTGGCTTGTGG-3' (sense) and 5'-CCCGAAGAGTTCGCGGAG-3' (antisense).

Assay for Transposase Accessible Chromatin (ATAC)

Chromatin accessibility at *BMPR1A* promoter region in the HCC cells was detected using the ATAC assay, which was conducted using the Hyperactive ATAC-Seq Library Prep Kit for Illumina (cat. no. TD711, Vazyme). The enriched *BMPR1A* promoter region was measured by qPCR using the primers 5'-TGTGGGGCTGGCTTGTGG-3' (sense) and 5'-CCCGAAGAGTTCGCGGAG-3' (antisense).

Statistical Analysis

Statistical analyses were performed using GraphPad Prism 6.0 Software. For the comparison of two groups, Student's *t*-test was performed. For the comparison of more than two groups, one-way ANOVA followed by Dunnett's multiple comparisons test was performed. Mann-Whitney test, Wilcoxon matched-pairs signed rank test, log-rank test, Student's *t*-test, one-way ANOVA followed by Dunnett's multiple comparisons test, and Spearman correlation analysis were also indicated in the figure legends. $P < 0.05$ was considered significant for all statistical analyses.

Results

NUTM2B-AS1 is an Oncofetal lncRNA in HCC

To investigate whether NUTM2B-AS1 is an oncofetal lncRNA in HCC, we collected four fetal and four adult liver tissues. The results revealed that NUTM2B-AS1 was significantly upregulated in fetal liver tissues compared to adult liver tissues (Figure 1A). The Cancer Genome Atlas (TCGA) Liver Hepatocellular Carcinoma (LIHC) data revealed that NUTM2B-AS1 was significantly upregulated in HCC tissues compared to noncancerous liver tissues (Figure 1B). Analysis of TCGA-LIHC data further revealed that NUTM2B-AS1 was highly expressed in HCC tissues with poor differentiation (Figure 1C), high α-fetoprotein (AFP) (Figure 1D), and large tumor size (Figure 1E). Analyses of TCGA-LIHC data using the online bioinformatics tool GEPIA (http://gepia.cancer-pku.cn/) showed that high NUTM2B-AS1 expression was associated with poor overall survival (Figure 1F). To confirm the expression pattern of NUTM2B-AS1 in HCC, we collected 60 pairs of HCC and matched noncancerous liver tissues. NUTM2B-AS1 was also highly expressed
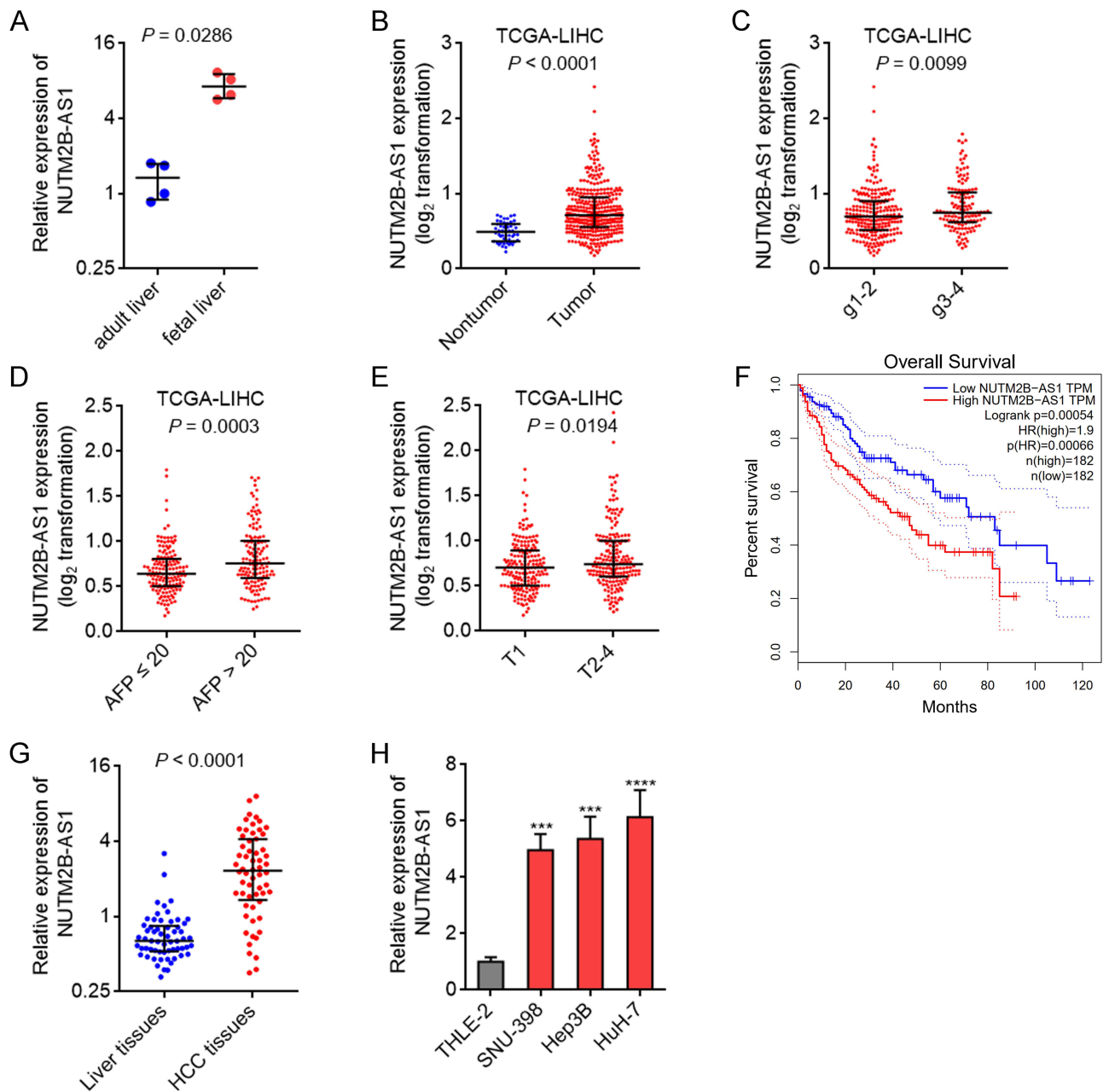
Figure 1 The oncofetal expression feature of NUTM2B-AS1 in HCC. (**A**) NUTM2B-AS1 expression in four fetal liver tissues and four adult liver tissues was measured by qPCR. (**B**) NUTM2B-AS1 expression in 50 normal liver tissues and 371 hCC tissues, according to TCGA LIHC data. (**C**) NUTM2B-AS1 expression in 232 hCC tissues with histologic grade 1–2 and 134 hCC tissues with histologic grade 3–4, according to TCGA LIHC data. (**D**) NUTM2B-AS1 expression in 147 hCC tissues with AFP value ≤ 20 and 131 hCC tissues with AFP value > 20, according to TCGA LIHC data. (**E**) NUTM2B-AS1 expression in 181 hCC tissues with pathologic T1 and 187 hCC tissues with pathologic T2-4, according to TCGA LIHC data. For A-E, *P* values were calculated by Mann-Whitney test. (**F**) The correlation between NUTM2B-AS1 expression and overall survival of HCC patients, according to TCGA LIHC data. (**G**) NUTM2B-AS1 expression in 60 pairs of HCC tissues and matched noncancerous liver tissues was measured by qPCR. *P* < 0.0001 by Wilcoxon matched-pairs signed rank test. (**H**) NUTM2B-AS1 expression in immortalized liver cell line THLE-2 and HCC cell lines SNU-398, Hep3B and HuH-7 was measured by qPCR. Results are shown as mean ± standard deviation (SD) of 3 independent experiments. ***P < 0.001, ****P < 0.0001 by one-way ANOVA followed by Dunnett's multiple comparisons test.

in HCC tissues compared to noncancerous liver tissues (Figure 1G). High NUTM2B-AS1 expression positively correlated with high AFP, poor differentiation, and advanced TNM stage (Supplementary Table 1). Furthermore, NUTM2B-AS1 was highly expressed in the HCC cell lines SNU-398, Hep3B, and HuH-7 compared to that in the immortalized noncancerous liver cell line THLE-2 (Figure 1H). These expression features suggested that NUTM2B-AS1 is an oncofetal lncRNA in HCC.

METTL3 and METTL16-Induced m⁶A Methylation of NUTM2B-AS1 Shows Oncofetal Feature

Two online bioinformatics tools RMBase 2.0 (https://rna.sysu.edu.cn/rmbase/m6Amod.php) and SRAMP (http://www.cuilab.cn/sramp), predicted NUTM2B-AS1 as an m⁶A modified transcript, with 70, 130, 568, 679, and 810 sites on NUTM2B-AS1 as predicted m⁶A sites. To investigate whether NUTM2B-AS1 was modified by m⁶A methylation, we performed MeRIP assays in the immortalized noncancerous liver cell line THLE-2 and HCC cell lines SNU-398, Hep3B, and HuH-7. The results revealed that NUTM2B-AS1 was m⁶A methylated in all cells, and that the m⁶A methylation level of NUTM2B-AS1 was higher in HCC cells than in immortalized noncancerous liver cell lines (Figure 2A). We randomly selected 20 pairs of HCC tissues and matched noncancerous liver tissues and performed MeRIP assays to detect m⁶A methylation levels of NUTM2B-AS1 in these tissues. The results revealed that the m⁶A methylation level of NUTM2B-AS1 was higher in HCC tissues than in non-cancerous liver tissues (Figure 2B). MeRIP assays in fetal and adult liver tissues showed that the m⁶A methylation level of NUTM2B-AS1 was higher in fetal liver tissues than in adult liver tissues (Figure 2C). These results suggest that the m⁶A methylation level of NUTM2B-AS1 exhibits oncofetal features. To confirm the m⁶A methylation sites on NUTM2B-AS1, we mutated the predicted 70, 130, 568, 679, and 810 sites on NUTM2B-AS1. MeRIP assays showed that only the mutation at 130 or 679 sites decreased the m⁶A methylation level of NUTM2B-AS1, and the concurrent mutation of 130 and 679 sites abolished m⁶A methylation of NUTM2B-AS1 (Figure 2D). These results showed that 130 and 679 sites were critical m⁶A methylation sites in NUTM2B-AS1, respectively. To identify the methyltransferases responsible for m⁶A methylation of NUTM2B-AS1, we analyzed the expression of methyltransferases METTL3, METTL14, METTL16, WTAP, and KIAA1429 in HCC and fetal liver tissues. TCGA-LIHC data revealed that METTL3 and METTL16 were significantly upregulated in HCC tissues compared with non-cancerous liver tissues (Figure 2E and F). Only METTL3 and METTL16 were also upregulated in fetal liver tissues compared to those in adult liver tissues (Figure 2G). MeRIP assays showed that ectopic expression of METTL3 or METTL16 increased the m⁶A methylation level of NUTM2B-AS1 (Figure 2H), whereas the depletion of METTL3 or METTL16 reduced the m⁶A methylation level of NUTM2B-AS1 (Figure 2I). These data suggest that METTL3- and METTL16-induced m⁶A methylation of NUTM2B-AS1 showed oncofetal features.

m⁶A Methylation Upregulates NUTM2B-AS1 via Increasing NUTM2B-AS1 Transcript Stability

Next, we investigated the effects of m⁶A methylation on NUTM2B-AS1 expression. Consistent with the change in the m⁶A methylation level of NUTM2B-AS1, ectopic expression of METTL3 or METTL16 also upregulated the expression of NUTM2B-AS1 (Figure 3A), whereas depletion of METTL3 or METTL16 reduced the expression of NUTM2B-AS1 (Figure 3B). m⁶A methylation has been frequently reported to modulate transcript stability.[46,47] We treated METTL3 or METTL16 overexpressed or silenced SNU-398 cells with α-amanitin to block new RNA generation and then detected the degradation of NUTM2B-AS1. The results revealed that Ectopic expression of METTL3 or METTL16 increased NUTM2B-AS1 transcript stability (Figure 3C), whereas the depletion of METTL3 or METTL16 reduced NUTM2B-AS1 transcript stability (Figure 3D). The m⁶A methylation level of NUTM2B-AS1 was positively correlated with its expression level in 20 randomly selected HCC tissues (Figure 3E). TCGA-LIHC data further showed that both METTL3 and METTL16 positively correlated with NUTM2B-AS1 expression in HCC tissues (Figure 3F and G). These data support the positive regulatory role of m⁶A methylation on NUTM2B-AS1 expression.

NUTM2B-AS1 Promotes HCC cellular Proliferation in an m⁶A-Dependent Manner

Given that both the expression and m⁶A methylation levels of NUTM2B-AS1 show oncofetal features, we studied the potential biological effects of NUTM2B-AS1 on HCC. We stably overexpressed wild-type (WT) or m⁶A methylation site-mutated NUTM2B-AS1 in SNU-398 cells with similar overexpression efficiency (Figure 4A). CCK-8 assay revealed that ectopic expression of WT, but not mutated NUTM2B-AS1, promoted SNU-398 cellular proliferation (Figure 4B). Stable over-expression of WT or m⁶A methylation site-mutated NUTM2B-AS1 in Hep3B cells with similar overexpression efficiencies
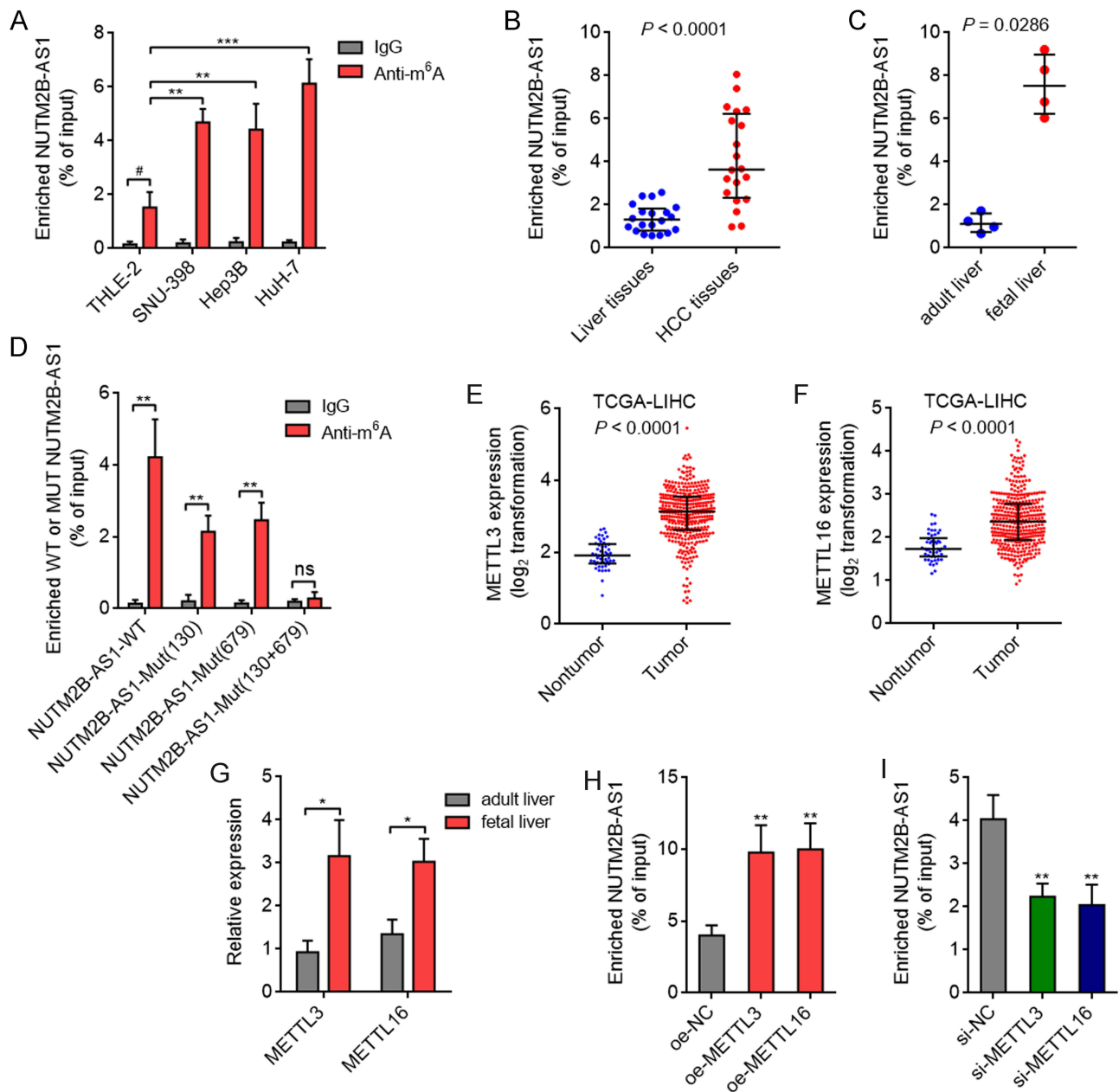
Figure 2 METTL3 and METTL16 induced m6A methylation of NUTM2B-AS1 shows oncofetal feature in HCC. (**A**) m6A methylation level of NUTM2B-AS1 in immortalized liver cell line THLE-2 and HCC cell lines SNU-398, Hep3B and HuH-7 was measured by MeRIP assays. Results are shown as mean ± SD of 3 independent experiments. ***P* < 0.01, ****P* < 0.001 by one-way ANOVA followed by Dunnett's multiple comparisons test. # *P* < 0.05 by Student's *t*-test. (**B**) m6A methylation level of NUTM2B-AS1 in 20 pairs of HCC tissues and matched noncancerous liver tissues was measured by MeRIP assays. *P* < 0.0001 by Wilcoxon matched-pairs signed rank test. (**C**) m6A methylation level of NUTM2B-AS1 in four fetal liver tissues and four adult liver tissues was measured by MeRIP assays. *P* = 0.0286 by Mann-Whitney test. (**D**) m6A methylation level of wild-type (WT) or mutated NUTM2B-AS1 was measured by MeRIP assays. (**E**) METTL3 expression in 50 normal liver tissues and 371 hCC tissues, according to TCGA LIHC data. *P* < 0.0001 by Mann-Whitney test. (**F**) METTL16 expression in 50 normal liver tissues and 371 hCC tissues, according to TCGA LIHC data. *P* < 0.0001 by Mann-Whitney test. (**G**) METTL3 and METTL16 expression in four fetal liver tissues and four adult liver tissues was measured by qPCR. (**H**) m6A methylation level of NUTM2B-AS1 in SNU-398 cells with METTL3 or METTL16 overexpression was measured by MeRIP assays. (**I**) m6A methylation level of NUTM2B-AS1 in SNU-398 cells with METTL3 or METTL16 depletion was measured by MeRIP assays. For (**D**) and (**G-I**), results are shown as mean ± SD of 3 independent experiments. **P* < 0.05, ***P* < 0.01, ns, not significant, by Student's *t*-test (**D**), Mann-Whitney test (**G**), or one-way ANOVA followed by Dunnett's multiple comparisons test (**H** and **I**).

also showed effects similar to those in SNU-398 cells (Figure 4C and D). EdU assays further confirmed the pro-proliferative role of WT but not mutated NUTM2B-AS1 in HCC cells (Figure 4E). Stable depletion of NUTM2B-AS1 reduced HuH-7 cellular proliferation, as evidenced by CCK-8 and EdU assays (Figure 4F–H). Overexpression of WT, but not mutated NUTM2B-AS1, rescued the reduced cell proliferation caused by NUTM2B-AS1 depletion (Supplementary Figure 1A and B).
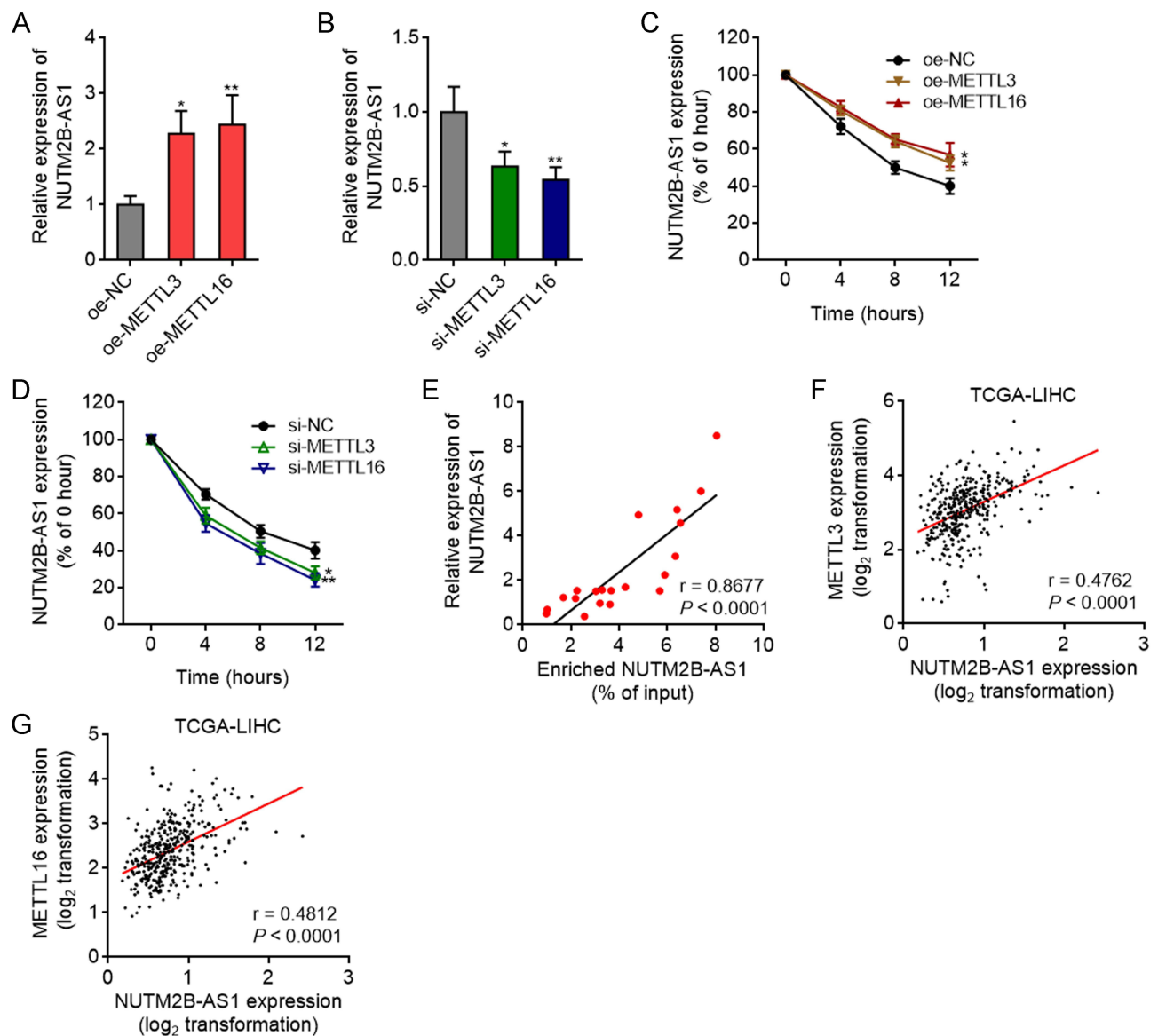
Figure 3 The effects of METTL3 and METTL16-mediated m⁶A methylation on NUTM2B-AS1. (**A**) NUTM2B-AS1 expression in SNU-398 cells with METTL3 or METTL16 overexpression was measured by qPCR. (**B**) NUTM2B-AS1 expression in SNU-398 cells with METTL3 or METTL16 depletion was measured by qPCR. (**C** and **D**) NUTM2B-AS1 transcript stability in SNU-398 cells with METTL3 or METTL16 overexpression (**C**) or depletion (**D**) over time was measured after blocking new RNA generation with α-amanitin (50 μM). For (**A-D**), results are shown as mean ± SD of 3 independent experiments. *$P < 0.05$, **$P < 0.01$ by one-way ANOVA followed by Dunnett's multiple comparisons test. (**E**) The correlation between expression level and m⁶A methylation level of NUTM2B-AS1 in 20 hCC tissues. (**F** and **G**) The correlation between NUTM2B-AS1 and METTL3 (**F**) or METTL16 (**G**) expression level in 371 hCC tissues, according to TCGA LIHC data. For (**E-G**), r and *P* values were calculated by Spearman correlation analysis.

NUTM2B-AS1 Enhances the Stemness Features of HCC in an m⁶A-Dependent Manner

Oncofetal genes have been reported to correlate with stem maintenance in malignancy.[6,48] Therefore, we investigated the effects of NUTM2B-AS1 on the stemness features of HCC. TCGA-LIHC data showed a positive correlation between the expression of NUTM2B-AS1 and well-known liver cancer stem cell markers, including CD24, CD44, CD133, CTNNB1, EPCAM, and NOTCH1 in HCC tissues (Figure 5A–F). Ectopic expression of WT, but not mutated NUTM2B-AS1, increased the expression of stem cell markers in SNU-398 and Hep3B cells (Figure 5G and H). NUTM2B-AS1 depletion decreased the expression of stem cell markers in HuH-7 cells (Figure 5I). Flow cytometry further confirmed that ectopic expression of WT, but not mutated NUTM2B-AS1, increased the protein expression of stem cell markers (Supplementary Figure 2A and B), and while NUTM2B-AS1 depletion decreased the protein expression of stem cell markers (Supplementary Figure 2C and D).
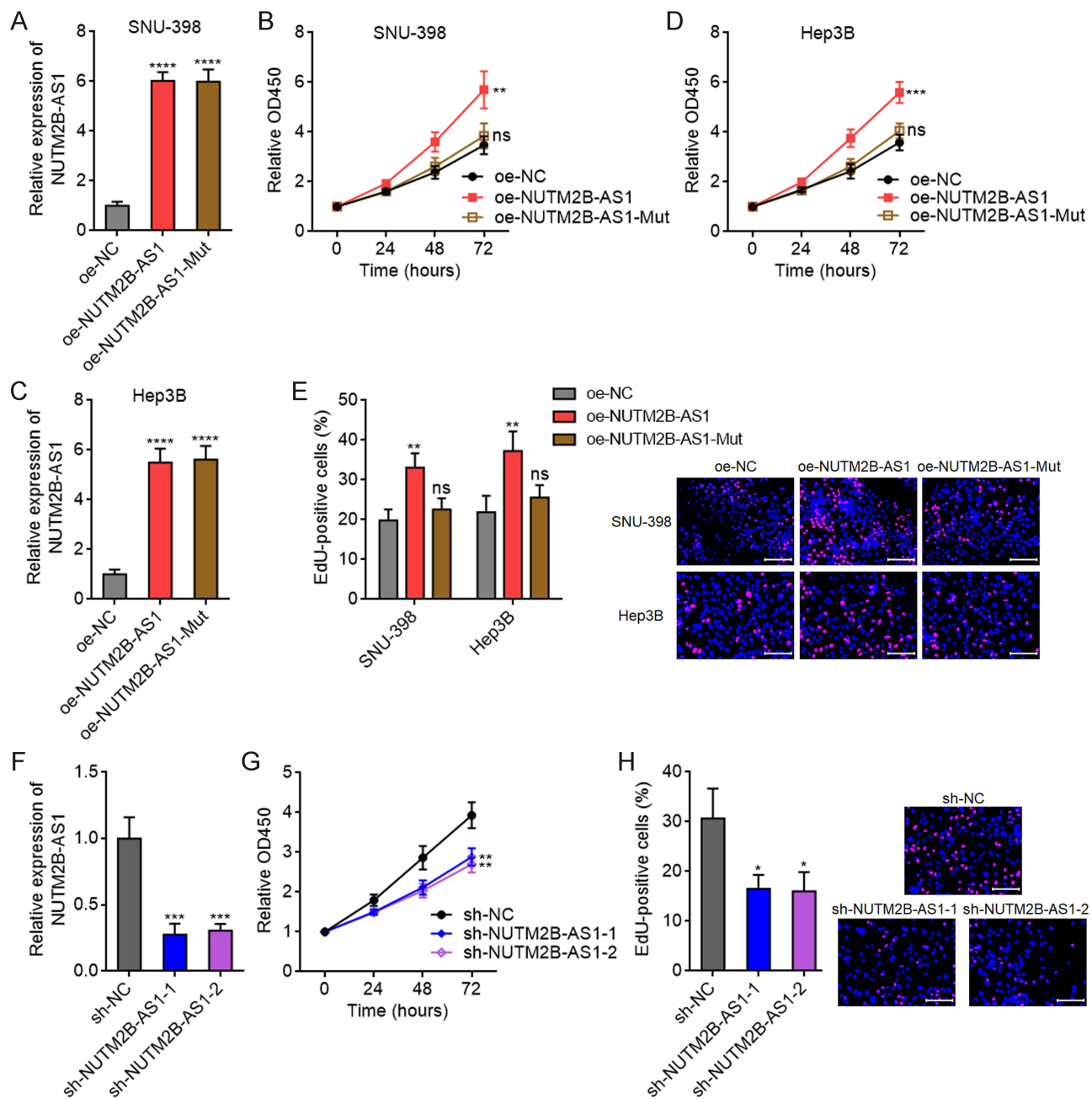
Figure 4 The effects of m⁶A-methylated NUTM2B-AS1 on HCC cellular proliferation. (**A**) NUTM2B-AS1 expression was measured by qPCR in SNU-398 cells with stable overexpression of wild type (WT) or m⁶A methylation sites mutated NUTM2B-AS1. (**B**) Cellular proliferation of SNU-398 cells with stable overexpression of WT or mutated NUTM2B-AS1 was measured by CCK-8 assays. (**C**) NUTM2B-AS1 expression was measured by qPCR in Hep3B cells with stable overexpression of WT or m⁶A methylation sites mutated NUTM2B-AS1. (**D**) Cellular proliferation of Hep3B cells with stable overexpression of WT or mutated NUTM2B-AS1 was measured by CCK-8 assays. (**E**) Cellular proliferation of SNU-398 and Hep3B cells with stable overexpression of WT or mutated NUTM2B-AS1 was measured by EdU assays. Scale bars, 100 μm. (**F**) NUTM2B-AS1 expression was measured by qPCR in HuH-7 cells with stable depletion of NUTM2B-AS1. (**G**) Cellular proliferation of HuH-7 cells with stable depletion of NUTM2B-AS1 was measured by CCK-8 assays. (**H**) Cellular proliferation of HuH-7 cells with stable depletion of NUTM2B-AS1 was measured by EdU assays. Scale bars, 100 μm. Results are shown as mean ± SD of 3 independent experiments. $*P < 0.05$, $**P < 0.01$, $***P < 0.001$, $****P < 0.0001$, ns, not significant, by one-way ANOVA followed by Dunnett's multiple comparisons test.

Sphere formation assays revealed that ectopic expression of WT, but not mutated NUTM2B-AS1, promoted the formation of tumor spheroids (Figure 5J), whereas depletion of NUTM2B-AS1 decreased the number of tumor spheroids (Figure 5K). Limiting dilution assays showed that SNU-398 cells with ectopic expression of WT, but not mutated NUTM2B-AS1, exhibited a significantly increased tumor-driving capacity in nude mice (Supplementary Figure 2E). These data suggested that NUTM2B-AS1 enhances the stemness of HCC cells.
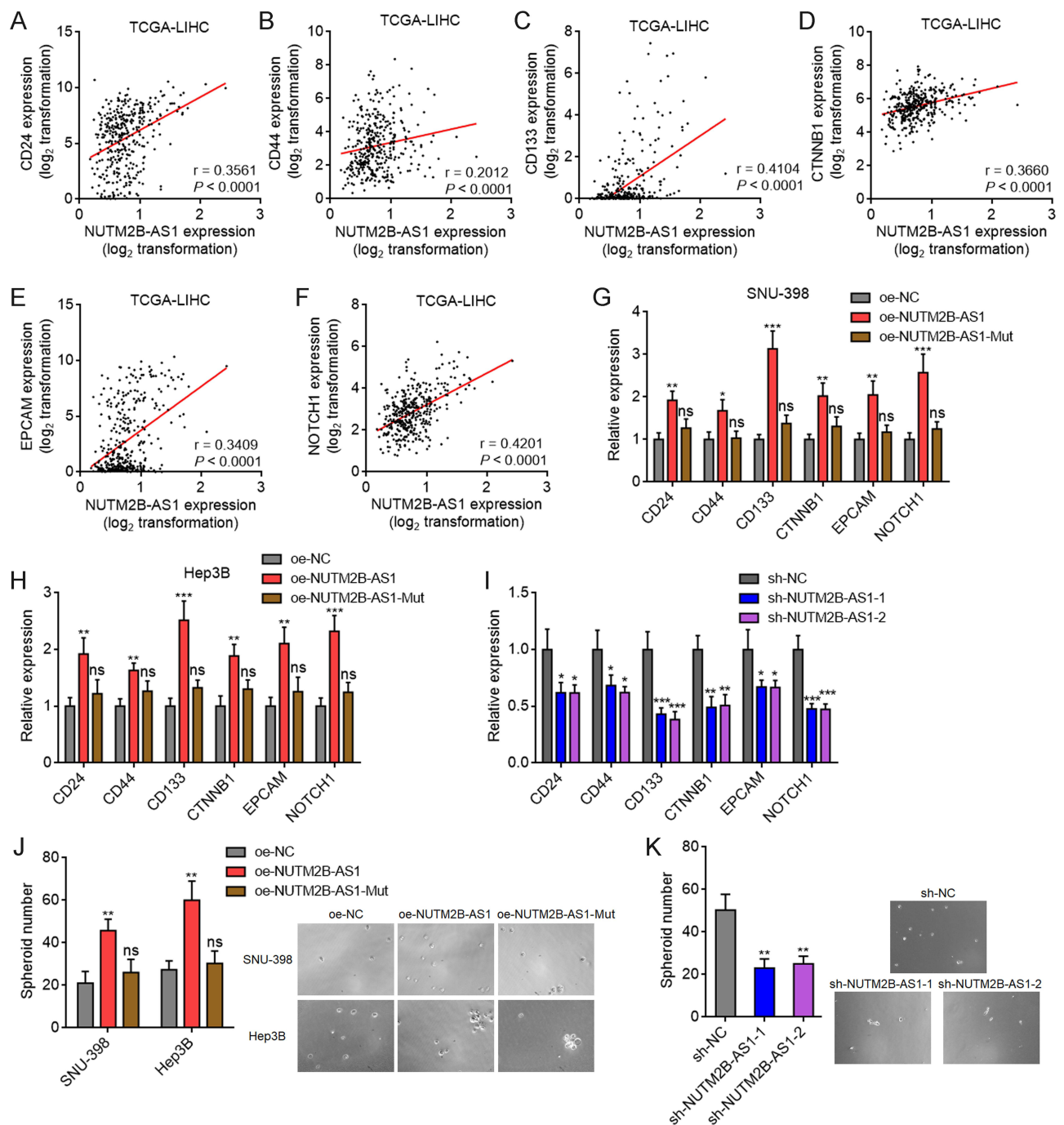
Figure 5 The effects of m⁶A-methylated NUTM2B-AS1 on stemness features of HCC. (**A-F**) The correlation between NUTM2B-AS1 and CD24 (**A**), CD44 (**B**), CD133 (**C**), CTNNB1 (**D**), EPCAM (**E**), or NOTCH1 (**F**) expression level in 371 hCC tissues, according to TCGA LIHC data. r and *P* values were calculated by Spearman correlation analysis. (**G and H**) Liver cancer stem cell markers CD24, CD44, CD133, CTNNB1, EPCAM, and NOTCH1 expression was measured by qPCR in SNU-398 (**G**) or Hep3B (**H**) cells with stable overexpression of WT or mutated NUTM2B-AS1. (**I**) Liver cancer stem cell markers CD24, CD44, CD133, CTNNB1, EPCAM, and NOTCH1 expression was measured by qPCR in HuH-7 cells with stable depletion of NUTM2B-AS1. (**J**) The spheroids form ability of SNU-398 and Hep3B cells with stable overexpression of WT or mutated NUTM2B-AS1. (**K**) The spheroids form ability of HuH-7 cells with stable depletion of NUTM2B-AS1. For (**G-K**), results are shown as mean ± SD of 3 independent experiments. *$P < 0.05$, **$P < 0.01$, ***$P < 0.001$, ns, not significant, by one-way ANOVA followed by Dunnett's multiple comparisons test.

NUTM2B-AS1 Upregulates BMPR1A Expression in an m⁶A-Dependent Manner

BMPR1A was identified as one of the most significantly correlated genes with NUTM2B-AS1 in HCC samples, analyzed by the online bioinformatics tool R2 Genomics Analysis and Visualization Platform (https://hgserver1.amc.nl/cgi-bin/r2/main.cgi), based on TCGA-LIHC data (Figure 6A). Consistent with the expression pattern of NUTM2B-AS1, BMPR1A was also
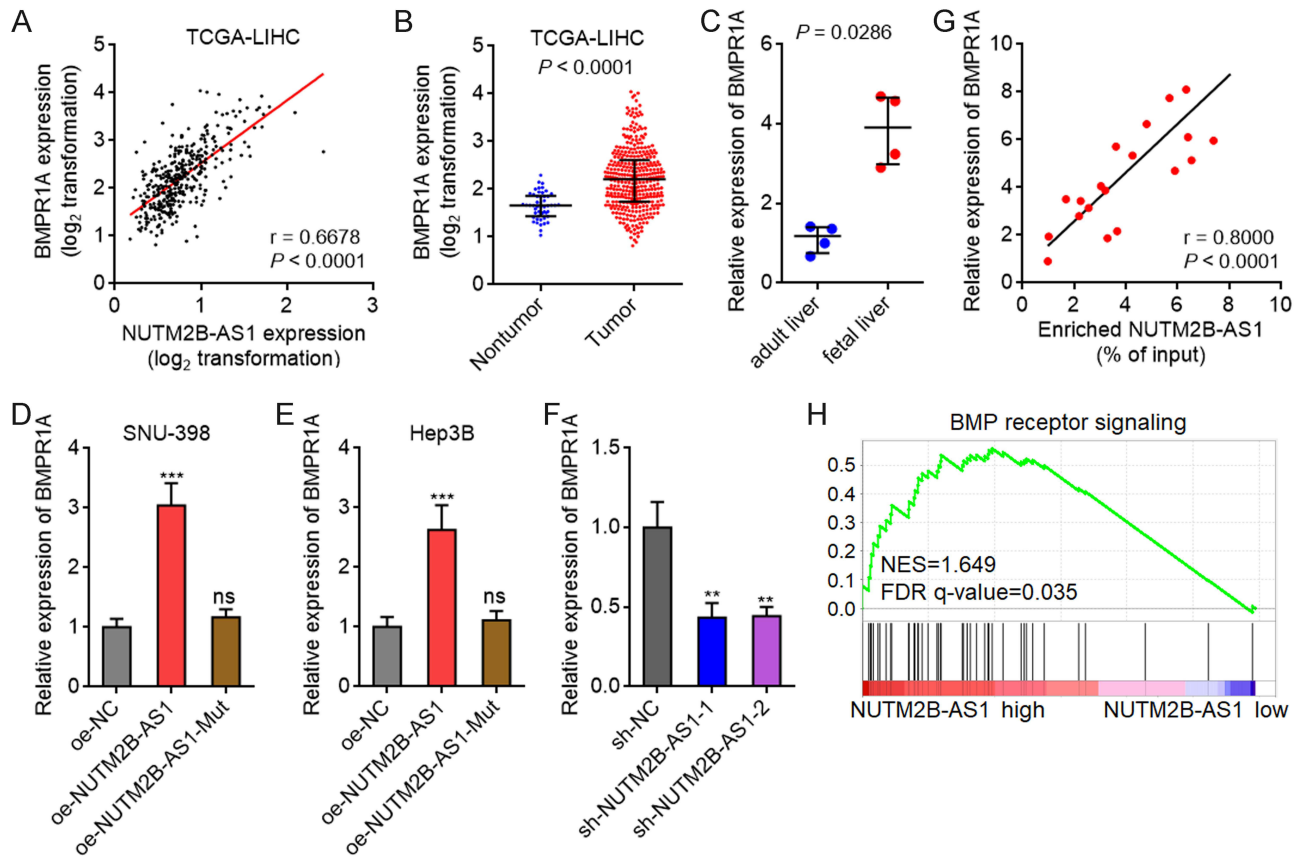
Figure 6 m⁶A-methylated NUTM2B-AS1 upregulated BMPR1A expression. (**A**) The correlation between BMPR1A and NUTM2B-AS1 expression level in 371 hCC tissues, according to TCGA LIHC data. r and P values were calculated by Spearman correlation analysis. (**B**) BMPR1A expression in 50 normal liver tissues and 371 hCC tissues, according to TCGA LIHC data. $P < 0.0001$ by Mann-Whitney test. (**C**) BMPR1A expression in four fetal liver tissues and four adult liver tissues was measured by qPCR. $P = 0.0286$ by Mann-Whitney test. (**D** and **E**) BMPR1A expression was measured by qPCR in SNU-398 (**D**) or Hep3B (**E**) cells with overexpression of WT or mutated NUTM2B-AS1. (**F**) BMPR1A expression was measured by qPCR in HuH-7 cells with depletion of NUTM2B-AS1. For (**D-F**), results are shown as mean ± SD of 3 independent experiments. **$P < 0.01$, ***$P < 0.001$, ns, not significant, by one-way ANOVA followed by Dunnett's multiple comparisons test. (**G**) The correlation between BMPR1A expression level and m⁶A methylation level of NUTM2B-AS1 in 20 hCC tissues. r and P values were calculated by Spearman correlation analysis. (**H**) GSEA of BMP receptor signaling in NUTM2B-AS1 high expression group versus NUTM2B-AS1 low expression group, according to TCGA LIHC data. NES, normalized enrichment score.

significantly upregulated in HCC tissues compared to noncancerous liver tissues (Figure 6B). Moreover, BMPR1A was significantly upregulated in fetal liver tissues compared to adult liver tissues (Figure 6C). Ectopic expression of WT, but not mutated NUTM2B-AS1, upregulated BMRP1A expression in both SNU-398 and Hep3B cells (Figure 6D and E). Depletion of NUTM2B-AS1 reduced BMRP1A expression (Figure 6F). These data suggest that NUTM2B-AS1 enhances BMPR1A expression in an m⁶A-dependent manner. The expression of BMPR1A was significantly positively correlated with the m⁶A methylation level of NUTM2B-AS1 in 20 randomly selected HCC tissue samples (Figure 6G). Gene set enrichment analysis (GSEA) of TCGA-LIHC data showed that Bone Morphogenetic Protein (BMP) receptor signaling was significantly enriched in the NUTM2B-AS1 high expression group (Figure 6H), which further supported the positive regulation of BMPR1A by NUTM2B-AS1.

m⁶A-Methylated NUTM2B-AS1 Upregulates H3K4me3 Modification and Augments Chromatin Accessibility at BMPR1A Promoter via Recruiting YTHDC2 and MLL1

To investigate the mechanisms underlying the regulation of BMPR1A by m⁶A-methylated NUTM2B-AS1, we first performed ChIRP assays, which revealed that NUTM2B-AS1 specifically binds to *BMPR1A* promoter (Figure 7A). Overexpression of WT or mutated NUTM2B-AS1 promoted enrichment of the *BMPR1A* promoter by NUTM2B-AS1 probes (Figure 7B), suggesting that both WT and mutated NUTM2B-AS1 bound to *BMPR1A* promoter. m⁶A-methylated transcripts have been reported to modulate histone modifications, including H3K9me2 and H3K4me3.[49,50] Therefore, we
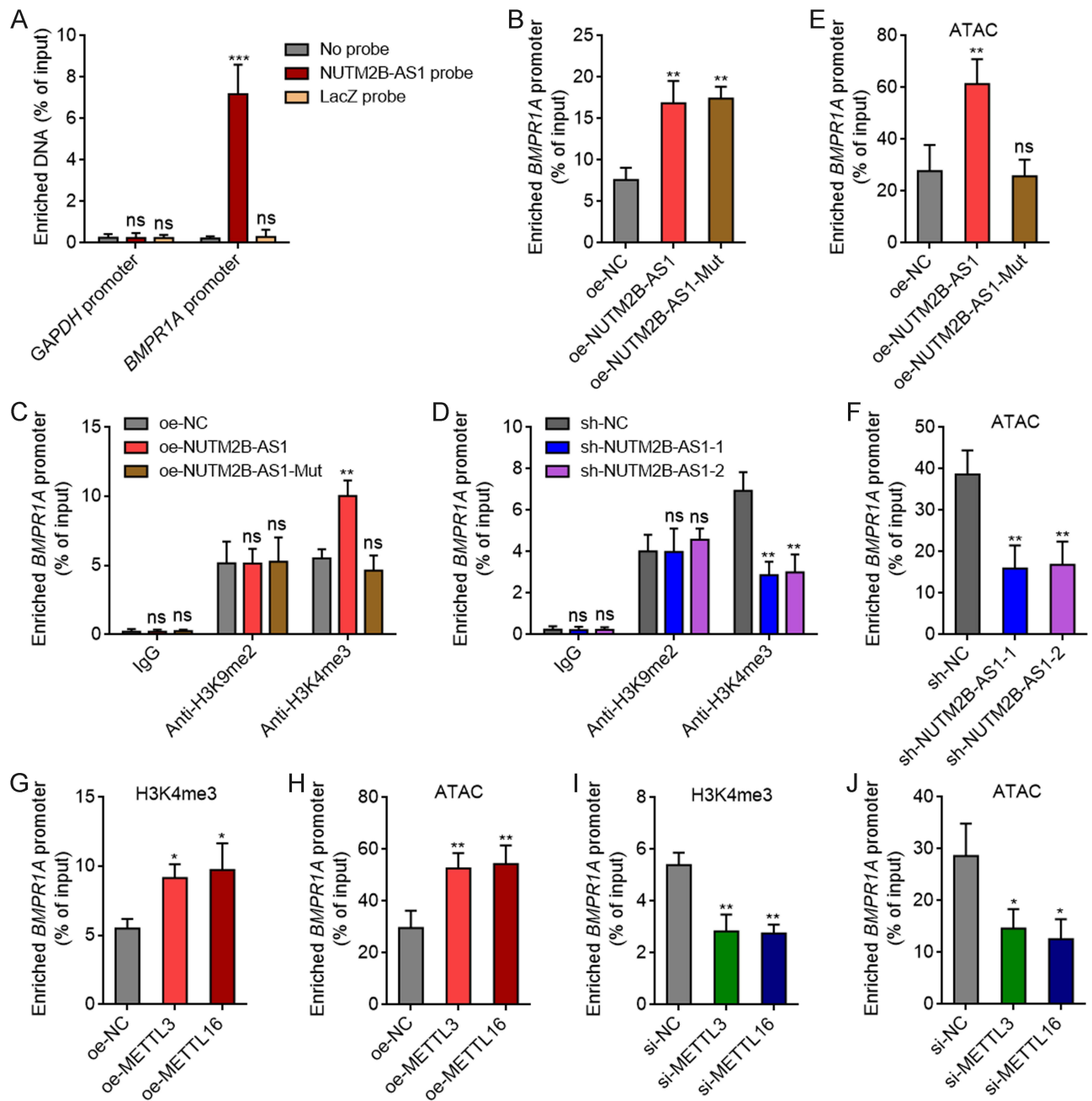
Figure 7 m⁶A-methylated NUTM2B-AS1 increased H3K4me3 modification and chromatin accessibility at *BMPR1A* promoter region. (**A**) ChIRP assays were performed to detect the binding of NUTM2B-AS1 to *BMPR1A* promoter region in SNU-398 cells. *GAPDH* promoter served as negative control. (**B**) ChIRP assays were performed to detect the binding of NUTM2B-AS1 to *BMPR1A* promoter region in SNU-398 cells with overexpression of WT or mutated NUTM2B-AS1. (**C**) ChIP assays were performed to detect H3K9me2 and H3K4me3 modification at *BMPR1A* promoter region in SNU-398 cells with overexpression of WT or mutated NUTM2B-AS1. (**D**) ChIP assays were performed to detect H3K9me2 and H3K4me3 modification at *BMPR1A* promoter region in HuH-7 cells with depletion of NUTM2B-AS1. (**E**) ATAC assays were performed to detect chromatin accessibility at *BMPR1A* promoter region in SNU-398 cells with overexpression of WT or mutated NUTM2B-AS1. (**F**) ATAC assays were performed to detect chromatin accessibility at *BMPR1A* promoter region in HuH-7 cells with depletion of NUTM2B-AS1. (**G**) ChIP assays were performed to detect H3K4me3 modification at *BMPR1A* promoter region in SNU-398 cells with overexpression of METTL3 or METTL16. (**H**) ATAC assays were performed to detect chromatin accessibility at *BMPR1A* promoter region in SNU-398 cells with overexpression of METTL3 or METTL16. (**I**) ChIP assays were performed to detect H3K4me3 modification at *BMPR1A* promoter region in SNU-398 cells with depletion of METTL3 or METTL16. (**J**) ATAC assays were performed to detect chromatin accessibility at *BMPR1A* promoter region in SNU-398 cells with depletion of METTL3 or METTL16. Results are shown as mean ± SD of 3 independent experiments. *$P < 0.05$, **$P < 0.01$, ***$P < 0.001$, ns, not significant, by one-way ANOVA followed by Dunnett's multiple comparisons test.

further investigated whether NUTM2B-AS1 influences histone modification at *BMPR1A* promoter region. ChIP assays showed that ectopic expression of WT, but not mutated NUTM2B-AS1, upregulated H3K4me3 modification at *BMPR1A* promoter region (Figure 7C). Neither WT nor mutated NUTM2B-AS1 affected H3K9me2 modifications in *BMPR1A*

promoter region (Figure 7C). NUTM2B-AS1 depletion reduced H3K4me3 modifications in *BMPR1A* promoter region (Figure 7D). ATAC assays revealed that ectopic expression of WT, but not mutated NUTM2B-AS1, augmented chromatin accessibility at *BMPR1A* promoter region (Figure 7E). NUTM2B-AS1 depletion reduced chromatin accessibility in *BMPR1A* promoter region (Figure 7F). Overexpression of METTL3 or METTL16, which induced m^{6}A methylation of NUTM2B-AS1, upregulated H3K4me3 modification and augmented chromatin accessibility in *BMPR1A* promoter region (Figure 7G and H). Depletion of METTL3 or METTL16 reduced H3K4me3 modification and chromatin accessibility in *BMPR1A* promoter region (Figure 7I and J).

m^{6}A-methylated super-enhancer RNAs have been reported to be recognized by m^{6}A reader YTHDC2, which further bound and recruited H3K4 methyltransferase MLL1 to upregulate H3K4me3 modification and augment chromatin accessibility.[50] Therefore, we further investigated whether m^{6}A-methylated NUTM2B-AS1 modulate BMPR1A in such a manner. RIP assays revealed that NUTM2B-AS1 bound to YTHDC2 and MLL1, which was enhanced by overexpression of METTL3 or METTL16 (Figure 8A). The depletion of METTL3 or METTL16 reduced the binding of NUTM2B-AS1 to YTHDC2 and MLL1 (Figure 8B). ChIP assays revealed that ectopic expression of WT, but not mutated NUTM2B-AS1, promoted the binding of YTHDC2 and MLL1 to *BMPR1A* promoter region (Figure 8C). Depletion of NUTM2B-AS1 decreased the binding of YTHDC2 and MLL1 to *BMPR1A* promoter region (Figure 8D). These data suggested that m^{6}A-methylated NUTM2B-AS1 binds and recruits YTHDC2 and MLL1 to *BMPR1A* promoter region. To investigate whether the regulation of BMPR1A by NUTM2B-AS1 was dependent on YTHDC2 and MLL1, we silenced YTHDC2 or MLL1 expression in NUTM2B-AS1 stably overexpressed SNU-398 cells and found that the depletion of YTHDC2 or MLL1 abolished the upregulation of BMPR1A by NUTM2B-AS1 (Figure 8E and F). TCGA-LIHC data showed a significant positive correlation between BMPR1A, YTHDC2, and MLL1 expression (Figure 8G and H), supporting the role of YTHDC2 and MLL1 in BMPR1A modulation. Collectively, these data suggest that m^{6}A-methylated NUTM2B-AS1 upregulates H3K4me3 modification and augments chromatin accessibility at *BMPR1A* promoter by recruiting YTHDC2 and MLL1.

Depletion of BMPR1A Reverses the Pro-Tumorigenic Roles of NUTM2B-AS1 in HCC

To explore whether the pro-tumorigenic role of NUTM2B-AS1 is dependent on the positive regulation of BMPR1A, we stably depleted BMPR1A in NUTM2B-AS1 overexpressed SNU-398 cells (Figure 9A). CCK-8 assays revealed that BMPR1A depletion abolished the pro-proliferative effects of NUTM2B-AS1 (Figure 9B). EdU assays further confirmed that BMPR1A depletion largely abolished the pro-proliferative role of NUTM2B-AS1 (Figure 9C). Sphere formation assays revealed that BMPR1A depletion largely abolished the role of NUTM2B-AS1 in increasing the number of tumor spheroids (Figure 9D). These data suggest that the role of NUTM2B-AS1 in promoting HCC cell proliferation and enhancing stemness is BMPR1A dependent.

Discussion

Fetal liver development and HCC carcinogenesis share many similar molecule features.[51] These oncofetal molecules are highly expressed in fetal liver and HCC, and silenced in adult normal liver tissues.[22] Some of these oncofetal molecules could be reliable biomarkers for HCC diagnosis and therapy, such as AFP and GPC3.[7,8] NUTM2B-AS1 was previously reported to be highly expressed and associated with poor prognosis in HCC.[52] However, we further identified NUTM2B-AS1 as an oncofetal lncRNA, which was increased in fetal liver and HCC tissues compared with adult noncancerous liver tissues. High expression of NUTM2B-AS1 was correlated with poor differentiation, high AFP, advanced stage, and poor prognosis. In addition to the expression level of NUTM2B-AS1, the m^{6}A methylation level of NUTM2B-AS1 was also found to present oncofetal characteristic. Our findings suggest that m^{6}A-methylated NUTM2B-AS1 is a novel oncofetal event. m^{6}A-methylated NUTM2B-AS1 in peripheral blood might represent another biomarker for early screening of HCC, which needs further investigations.

Our finding revealed that the m^{6}A methylation of NUTM2B-AS1 was induced by m^{6}A methyltransferases METTL3 and METTL16. The expression of METTL3 and METTL16 also showed oncofetal characteristic. METTL3 has been reported to play oncogenic roles in HCC by modulating various targets.[53,54] NUTM2B-AS1 was identified as another target of METTL3. METTL16 is located in both the nucleus and cytosol.[55,56] Nuclear METTL16 was reported to mainly function
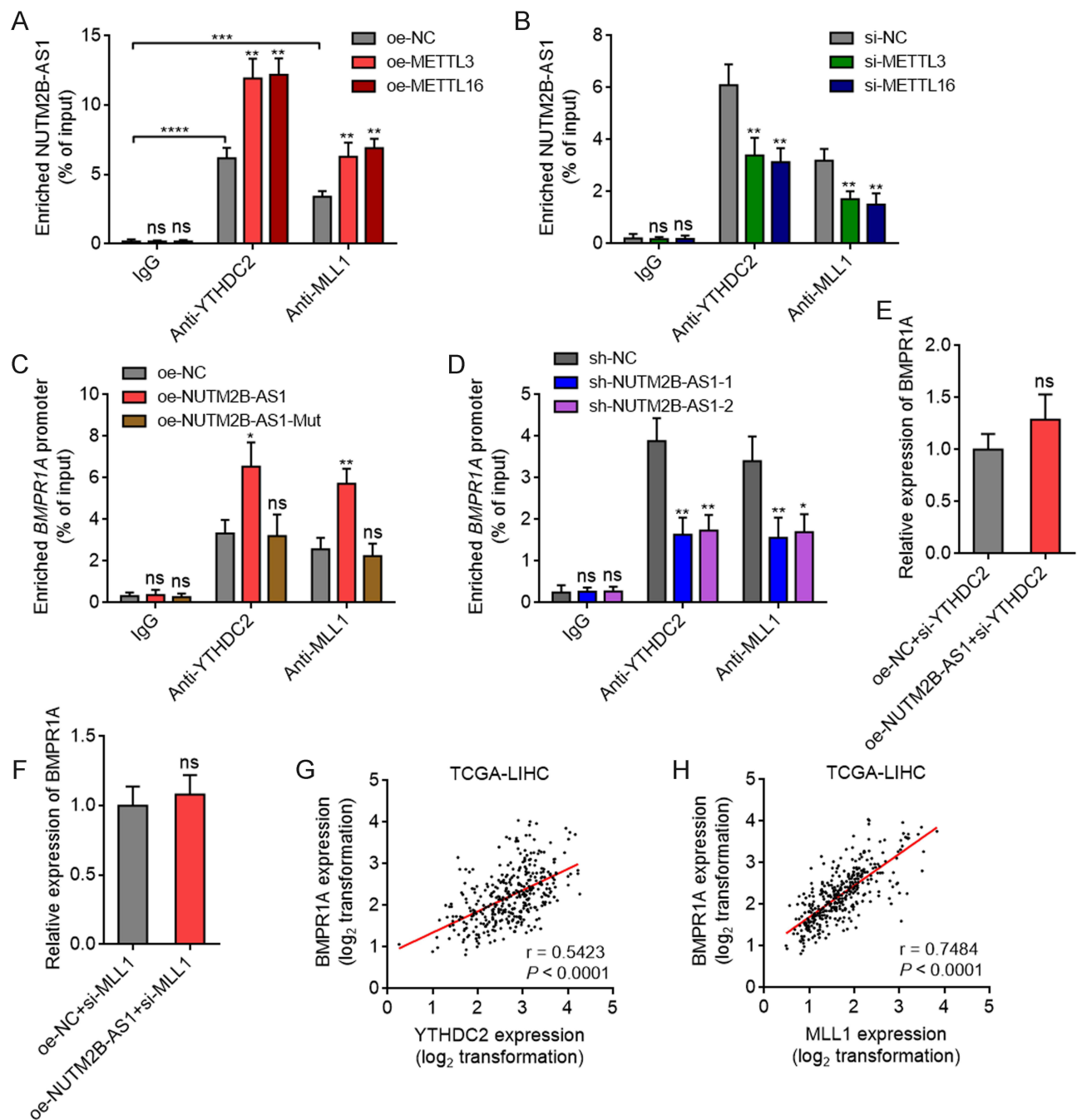
Figure 8 m^{6}A-methylated NUTM2B-AS1 bound and recruited YTHDC2 and MLL1 to *BMPR1A* promoter region to activate *BMPR1A* expression. (**A**) RIP assays were performed to detect the binding of NUTM2B-AS1 to YTHDC2 and MLL1 in SNU-398 cells with overexpression of METTL3 or METTL16. (**B**) RIP assays were performed to detect the binding of NUTM2B-AS1 to YTHDC2 and MLL1 in SNU-398 cells with depletion of METTL3 or METTL16. (**C**) ChIP assays were performed to detect the binding of YTHDC2 and MLL1 to *BMPR1A* promoter region in SNU-398 cells with overexpression of WT or mutated NUTM2B-AS1. (**D**) ChIP assays were performed to detect the binding of YTHDC2 and MLL1 to *BMPR1A* promoter region in SNU-398 cells with depletion of NUTM2B-AS1. (**E**) BMPR1A expression was measured by qPCR in SNU-398 cells with concurrent overexpression of NUTM2B-AS1 and depletion of YTHDC2. (**F**) BMPR1A expression was measured by qPCR in SNU-398 cells with concurrent overexpression of NUTM2B-AS1 and depletion of MLL1. (**G** and **H**) The correlation between BMPR1A and YTHDC2 (**G**) or MLL1 (**H**) expression level in 371 hCC tissues, according to TCGA LIHC data. r and *P* values were calculated by Spearman correlation analysis. For (**A-F**), results are shown as mean ± SD of 3 independent experiments. *$P < 0.05$, **$P < 0.01$, ***$P < 0.001$, ****$P < 0.0001$, ns, not significant, by one-way ANOVA followed by Dunnett's multiple comparisons test (**A-D**) or Student's *t*-test (**E** and **F**).

as an m^{6}A writer, and while cytosolic METTL16 was reported to promote translation in an m^{6}A-independent manner.[56] We observed that METTL16 functions as an m^{6}A writer to install m^{6}A on NUTM2B-AS1. Many previous reports have shown that m^{6}A methylation modulates transcript stability.[57,58] Consistent with this, m^{6}A methylation increased NUTM2B-AS1
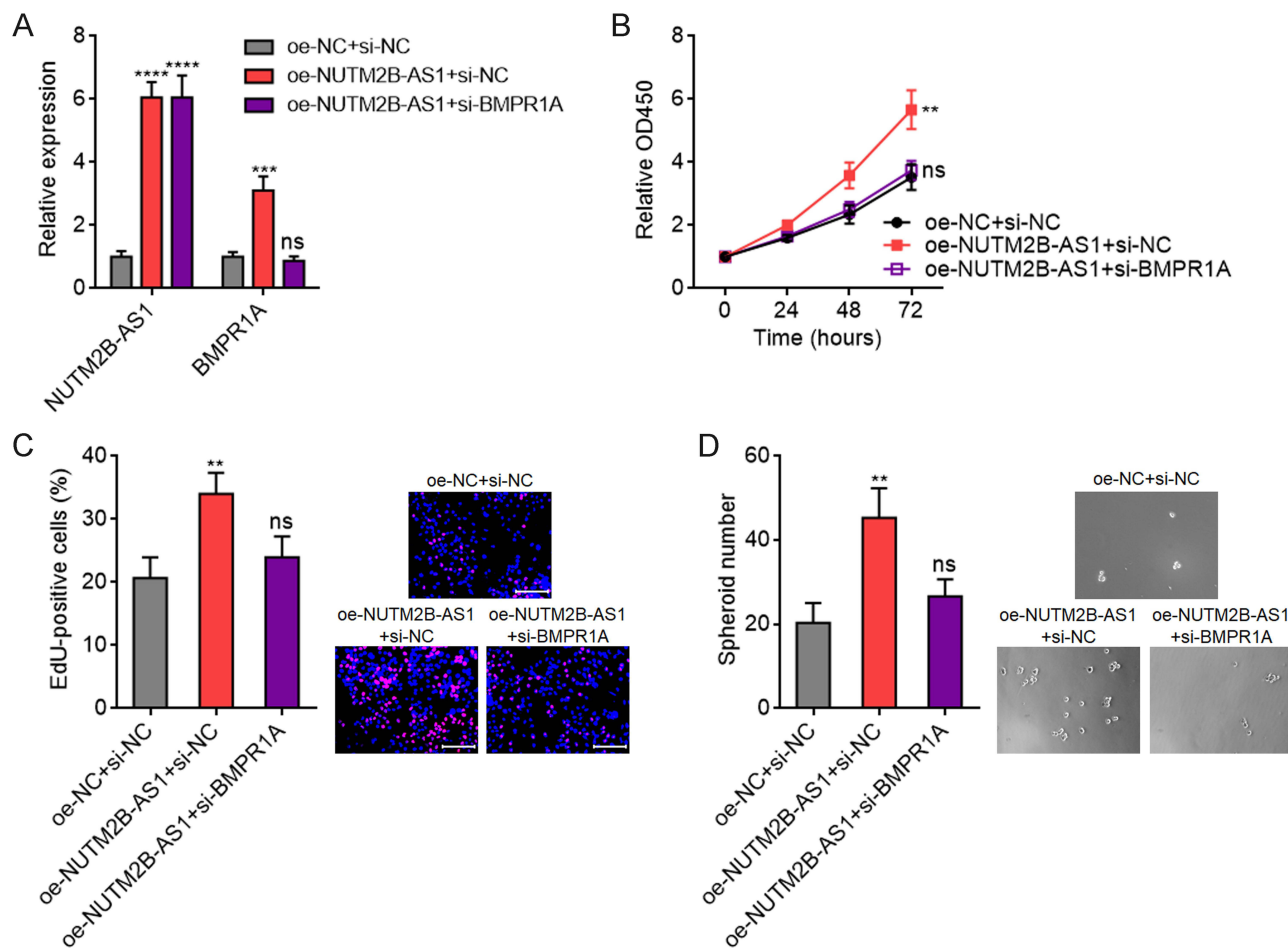
Figure 9 The oncogenic roles of NUTM2B-AS1 in HCC were dependent on BMPR1A. (**A**) NUTM2B-AS1 and BMPR1A expression was measured by qPCR in SNU-398 cells with concurrent overexpression of NUTM2B-AS1 and depletion of BMPR1A. (**B**) Cellular proliferation of SNU-398 cells with concurrent overexpression of NUTM2B-AS1 and depletion of BMPR1A was measured by CCK-8 assays. (**C**) Cellular proliferation of SNU-398 cells with concurrent overexpression of NUTM2B-AS1 and depletion of BMPR1A was measured by EdU assays. Scale bars, 100 μm. (**D**) The spheroids form ability of SNU-398 cells with concurrent overexpression of NUTM2B-AS1 and depletion of BMPR1A. Results are shown as mean ± SD of 3 independent experiments. **$P < 0.01$, ***$P < 0.001$, ****$P < 0.0001$, ns, not significant, by one-way ANOVA followed by Dunnett's multiple comparisons test.

transcript stability, leading to upregulation of NUTM2B-AS1. Our findings suggest that METTL3/METTL16-induced m[6]A methylation of NUTM2B-AS1 increased NUTM2B-AS1 expression. METTL3, METTL16, m[6]A methylation level of NUTM2B-AS1, and expression level of NUTM2B-AS1 all represent oncofetal molecular events.

Intriguingly, functional assays showed that only m[6]A-methylated NUTM2B-AS1 promoted HCC cell proliferation and enhanced HCC cellular stemness features, which was consistent with the oncofetal characteristic of the m[6]A methylation level of NUTM2B-AS1. Thus, our findings suggested that m[6]A-methylated NUTM2B-AS1 is a functional oncofetal event in HCC.

Mechanistic investigations identified BMPR1A as a downstream target of NUTM2B-AS1. BMPR1A is a bone morphogenetic protein (BMP) receptor that delivers and activates BMP signaling.[40] Previous studies have found that BMP signaling plays an important role in stem cell differentiation and self-renewal.[41,42] In this study, our findings confirmed that BMPR1A was a critical mediator of the oncogenic roles of m[6]A-methylated NUTM2B-AS1 in HCC. We observed that the m[6]A reader YTHDC2 recognized and interacted with m[6]A-methylated NUTM2B-AS1, which also bound to the *BMPR1A* promoter region. Therefore, m[6]A-methylated NUTM2B-AS1 recruited YTHDC2 to *BMPR1A* promoter region. YTHDC2 further bound and recruited H3K4 methyltransferase MLL1 to *BMPR1A* promoter region. Thus, m[6]A-methylated NUTM2B-AS1 increased H3K4me3 modification and chromatin accessibility at *BMPR1A* promoter region. In our previous studies, we have found that m[6]A-methylated

transcripts regulating H3K9me2 at the promoters of target genes.[59,60] The current study provides novel evidence for the role of m^{6}A methylation in epigenetic modulation of gene transcription.

Conclusion

In conclusion, this study revealed that METTL3- and METTL16-induced m^{6}A methylation of NUTM2B-AS1 was a novel oncofetal molecular event in HCC. m^{6}A-methylated NUTM2B-AS1 promotes HCC cell proliferation and enhances HCC cellular stemness by upregulating BMPR1A. m^{6}A-methylated NUTM2B-AS1 binds and recruits YTHDC2 and MLL1 to *BMPR1A* promoter region to increase H3K4me3 modification and chromatin accessibility at *BMPR1A* promoter region, leading to transcriptional activation of *BMPR1A*. m^{6}A methylation of NUTM2B-AS1 represents a novel therapeutic target for HCC.

Abbreviations

HCC, Hepatocellular carcinoma; m^{6}A, N^6-methyladenosine; RIP, RNA immunoprecipitation; ChIRP, Chromatin isolation by RNA purification; ChIP, Chromatin immunoprecipitation; ATAC, assay for transposase-accessible chromatin; lncRNA, long noncoding RNA; TCGA, The Cancer Genome Atlas; LIHC, liver hepatocellular carcinoma; qPCR, quantitative polymerase chain reaction; NC, negative control; CCK-8, Cell Counting Kit-8; EdU,5-ethynyl-2'-deoxyuridine; MeRIP, methylated RNA immunoprecipitation; AFP, α-fetoprotein; WT, wild-type; GSEA, gene set enrichment analysis.

Ethical Approval and Consent to Participate

This study was conducted in accordance with the 1964 helsinki Declaration and approved by the Affiliated Hospital of Youjiang Medical University for Nationalities Institutional Review Board. Written informed consent was obtained from all participants.

Funding

Disclosure

The authors report no conflicts of interest in this work.

References

1. Qi J, Li M, Wang L, et al. National and subnational trends in cancer burden in China, 2005-20: an analysis of national mortality surveillance data. *Lancet Public Health*. 2023;8:e943–e955. doi:10.1016/S2468-2667(23)00211-6
2. Siegel RL, Miller KD, Wagle NS, Jemal A. Cancer statistics, 2023. *CA Cancer J Clin*. 2023;73:17–48. doi:10.3322/caac.21763
3. Llovet JM, Kelley RK, Villanueva A, et al. Hepatocellular carcinoma. *Nat Rev Dis Primers*. 2021;7:6. doi:10.1038/s41572-020-00240-3
4. Villanueva A. Hepatocellular Carcinoma. *N Engl J Med*. 2019;380:1450–1462. doi:10.1056/NEJMra1713263
5. Liang R, Hong W, Zhang Y, et al. Deep dissection of stemness-related hierarchies in hepatocellular carcinoma. *J Transl Med*. 2023;21:631. doi:10.1186/s12967-023-04425-8
6. Sharma A, Bleriot C, Currenti J, Ginhoux F. Oncofetal reprogramming in tumour development and progression. *Nat Rev Cancer*. 2022;22:593–602. doi:10.1038/s41568-022-00497-8
7. Lu SX, Huang YH, Liu LL, et al. alpha-Fetoprotein mRNA in situ hybridisation is a highly specific marker of hepatocellular carcinoma: a multi-centre study. *Br J Cancer*. 2021;124:1988–1996. doi:10.1038/s41416-021-01363-4
8. Filmus J, Capurro M. Glypican-3: a marker and a therapeutic target in hepatocellular carcinoma. *FEBS J*. 2013;280:2471–2476. doi:10.1111/febs.12126
9. Yong KJ, Gao C, Lim JS, et al. Oncofetal gene SALL4 in aggressive hepatocellular carcinoma. *N Engl J Med*. 2013;368:2266–2276. doi:10.1056/NEJMoa1300297
10. Yuan JH, Liu XN, Wang TT, et al. The MBNL3 splicing factor promotes hepatocellular carcinoma by increasing PXN expression through the alternative splicing of lncRNA-PXN-AS1. *Nat Cell Biol*. 2017;19:820–832. doi:10.1038/ncb3538
11. Gamaev L, Mizrahi L, Friehmann T, et al. The pro-oncogenic effect of the lncRNA H19 in the development of chronic inflammation-mediated hepatocellular carcinoma. *Oncogene*. 2021;40:127–139. doi:10.1038/s41388-020-01513-7
12. Li J, Li MH, Wang TT, et al. SLC38A4 functions as a tumour suppressor in hepatocellular carcinoma through modulating Wnt/beta-catenin/MYC/HMGCS2 axis. *Br J Cancer*. 2021;125:865–876. doi:10.1038/s41416-021-01490-y

13. Barajas-Mora EM, Lee L, Lu H, et al. Enhancer-instructed epigenetic landscape and chromatin compartmentalization dictate a primary antibody repertoire protective against specific bacterial pathogens. *Nat Immunol*. 2023;24:320–336. doi:10.1038/s41590-022-01402-z

14. Liang WW, Lu RJ, Jayasinghe RG, et al. Integrative multi-omic cancer profiling reveals DNA methylation patterns associated with therapeutic vulnerability and cell-of-origin. *Cancer Cell*. 2023;41:1567–1585e7. doi:10.1016/j.cell.2023.07.013

15. Shirvaliloo M, Akhavan-Sigari R. Epigenetic cues regulating airway development in human lung organoids: polycomb repressive complex 2 and altered chromatin accessibility determine cell fate. *FASEB J*. 2023;37:e22868. doi:10.1096/fj.202201666R

16. Han L, Huang D, Wu S, et al. Lipid droplet-associated lncRNA LIPTER preserves cardiac lipid metabolism. *Nat Cell Biol*. 2023;25:1033–1046. doi:10.1038/s41556-023-01162-4

17. Wen R, Zhang TN, Zhang T, et al.. A novel long noncoding RNA-lncRNA-AABR07066529.3 alleviates inflammation, apoptosis, and pyroptosis by inhibiting MyD88 in lipopolysaccharide-induced myocardial depression. *FASEB J*. 2023;37:e23063. doi:10.1096/fj.202201680R

18. Zhao T, Sun Z, Lai X, et al. Tamoxifen exerts anti-peritoneal fibrosis effects by inhibiting H19-activated VEGFA transcription. *J Transl Med*. 2023;21:614. doi:10.1186/s12967-023-04470-3

19. Yuan JH, Yang F, Wang F, et al. A long noncoding RNA activated by TGF-beta promotes the invasion-metastasis cascade in hepatocellular carcinoma. *Cancer Cell*. 2014;25:666–681. doi:10.1016/j.ccr.2014.03.010

20. Liu L, Yang X, Zhang J, et al.. Long non-coding RNA SNHG11 regulates the Wnt/beta-catenin signaling pathway through rho/ROCK in trabecular meshwork cells. *FASEB J*. 2023:37:e22873. doi:10.1096/fj.202201733RRR

21. Li Y, Ding T, Hu H, et al. LncRNA-ATB participates in the regulation of calcium oxalate crystal-induced renal injury by sponging the miR-200 family. *Mol Med*. 2021;27:143. doi:10.1186/s10020-021-00403-2

22. Wang F, Yuan JH, Wang SB, et al. Oncofetal long noncoding RNA PVT1 promotes proliferation and stem cell-like property of hepatocellular carcinoma cells by stabilizing NOP2. *Hepatology*. 2014;60:1278–1290. doi:10.1002/hep.27239

23. Zhu Y, Xiao B, Liu M, et al. N6-methyladenosine-modified oncofetal lncRNA MIR4435-2HG contributed to stemness features of hepatocellular carcinoma cells by regulating rRNA 2'-O methylation. *Cell Mol Biol Lett*. 2023;28:89. doi:10.1186/s11658-023-00493-2

24. Zhang Y, Zhang W, Zhao J, et al. m(6)A RNA modification regulates innate lymphoid cell responses in a lineage-specific manner. *Nat Immunol*. 2023;24:1256–1264. doi:10.1038/s41590-023-01548-4

25. Collignon E, Cho B, Furlan G, et al. m(6)A RNA methylation orchestrates transcriptional dormancy during paused pluripotency. *Nat Cell Biol*. 2023;25:1279–1289. doi:10.1038/s41556-023-01212-x

26. Tang Q, Li L, Wang Y, et al. RNA modifications in cancer. *Br J Cancer*. 2023;129:204–221. doi:10.1038/s41416-023-02275-1

27. Luo Y, Chen J, Cui Y, et al.. Transcriptome-wide high-throughput m(6) A sequencing of differential m(6) A methylation patterns in the decidual tissues from RSA patients. *FASEB J*. 2023;37:e22802. doi:10.1096/fj.202201232RRRR

28. Wang L, Dou X, Chen S, et al. YTHDF2 inhibition potentiates radiotherapy antitumor efficacy. *Cancer Cell*. 2023;41:1294–1308e8. doi:10.1016/j.ccell.2023.04.019

29. Zhao L, Liu Y, Ma B, Liu X, Wei R, Nian H. METTL3 inhibits autoreactive Th17 cell responses in experimental autoimmune uveitis via stabilizing ASH1L mRNA. *FASEB J*. 2023;37:e22803. doi:10.1096/fj.202201548R

30. Ito-Kureha T, Leoni C, Borland K, et al. The function of Wtap in N(6)-adenosine methylation of mRNAs controls T cell receptor signaling and survival of T cells. *Nat Immunol*. 2022;23:1208–1221. doi:10.1038/s41590-022-01268-1

31. Dai YZ, Liu YD, Li J, et al. METTL16 promotes hepatocellular carcinoma progression through downregulating RAB11B-AS1 in an m(6) A-dependent manner. *Cell Mol Biol Lett*. 2022;27:41. doi:10.1186/s11658-022-00342-8

32. Kobayashi R, Kawabata-Iwakawa R, Terakawa J, et al.. Aberrant activation of estrogen receptor-alpha signaling in Mettl14-deficient uteri impairs embryo implantation. *FASEB J*. 2023;37:e23093. doi:10.1096/fj.202300735R

33. Mansfield KD. RNA Binding by the m6A Methyltransferases METTL16 and METTL3. *Biology*. 2024;13:doi:10.3390/biology13060391.

34. Wu S, Tang W, Liu L, et al. Obesity-induced downregulation of miR-192 exacerbates lipopolysaccharide-induced acute lung injury by promoting macrophage activation. *Cell Mol Biol Lett*. 2024;29:36. doi:10.1186/s11658-024-00558-w

35. Xu C, Zhou J, Zhang X, et al. N(6)-methyladenosine-modified circ_104797 sustains cisplatin resistance in bladder cancer through acting as RNA sponges. *Cell Mol Biol Lett*. 2024;29:28. doi:10.1186/s11658-024-00543-3

36. Ye M, Chen J, Yu P, et al.. WTAP activates MAPK signaling through m6A methylation in VEGFA mRNA-mediated by YTHDC1 to promote colorectal cancer development. *FASEB J*. 2023;37:e23090. doi:10.1096/fj.202300344RRR

37. Weng H, Huang F, Yu Z, et al. The m(6)A reader IGF2BP2 regulates glutamine metabolism and represents a therapeutic target in acute myeloid leukemia. *Cancer Cell*. 2022;40:1566–1582e10. doi:10.1016/j.ccell.2022.10.004

38. Jiang T, He X, Zhao Z, Zhang X, Wang T, Jia L. RNA m6A reader IGF2BP3 promotes metastasis of triple-negative breast cancer via SLIT2 repression. *FASEB J*. 2022;36:e22618. doi:10.1096/fj.202200751RR

39. Shimura T, Kandimalla R, Okugawa Y, et al. Novel evidence for m(6)A methylation regulators as prognostic biomarkers and FTO as a potential therapeutic target in gastric cancer. *Br J Cancer*. 2022;126:228–237. doi:10.1038/s41416-021-01581-w

40. Voeltzel T, Flores-Violante M, Zylbersztejn F, et al. A new signaling cascade linking BMP4, BMPR1A, DeltaNp73 and NANOG impacts on stem-like human cell properties and patient outcome. *Cell Death Dis*. 2018;9:1011. doi:10.1038/s41419-018-1042-7

41. Wang Y, Zhu P, Luo J, et al.. LncRNA HAND2-AS1 promotes liver cancer stem cell self-renewal via BMP signaling. *EMBO J*. 2019:38:e101110. doi:10.15252/embj.2018101110

42. Saadey AA, Yousif A, Osborne N, et al. Rebalancing TGFbeta1/BMP signals in exhausted T cells unlocks responsiveness to immune checkpoint blockade therapy. *Nat Immunol*. 2023;24:280–294. doi:10.1038/s41590-022-01384-y

43. Wei H, Xu Z, Chen L, et al. Long non-coding RNA PAARH promotes hepatocellular carcinoma progression and angiogenesis via upregulating HOTTIP and activating HIF-1alpha/VEGF signaling. *Cell Death Dis*. 2022;13:102. doi:10.1038/s41419-022-04505-5

44. Pu J, Xu Z, Huang Y, et al. N(6) -methyladenosine-modified FAM111A-DT promotes hepatocellular carcinoma growth via epigenetically activating FAM111A. *Cancer Sci*. 2023;114:3649–3665. doi:10.1111/cas.15886

45. Li J, Liu XG, Ge RL, et al. The ligation between ERMAP, galectin-9 and dectin-2 promotes Kupffer cell phagocytosis and antitumor immunity. *Nat Immunol*. 2023;24:1813–1824. doi:10.1038/s41590-023-01634-7

46. Chen X, Lu T, Cai Y, et al. KIAA1429-mediated m6A modification of CHST11 promotes progression of diffuse large B-cell lymphoma by regulating Hippo-YAP pathway. *Cell Mol Biol Lett*. 2023;28:32. doi:10.1186/s11658-023-00445-w

2410

Journal of Hepatocellular Carcinoma 2024:11

47. Chen J, Ye M, Bai J, et al. ALKBH5 enhances lipid metabolism reprogramming by increasing stability of FABP5 to promote pancreatic neuroendocrine neoplasms progression in an m6A-IGF2BP2-dependent manner. *J Transl Med*. 2023;21:741. doi:10.1186/s12967-023-04578-6

48. Simon AG, Lyu SI, Laible M, et al. The tight junction protein claudin 6 is a potential target for patient-individualized treatment in esophageal and gastric adenocarcinoma and is associated with poor prognosis. *J Transl Med*. 2023;21:552. doi:10.1186/s12967-023-04433-8

49. Li Y, Xia L, Tan K, et al. N(6)-Methyladenosine co-transcriptionally directs the demethylation of histone H3K9me2. *Nat Genet*. 2020;52:870–877. doi:10.1038/s41588-020-0677-3

50. Li R, Zhao H, Huang X, et al. Super-enhancer RNA m(6)A promotes local chromatin accessibility and oncogene transcription in pancreatic ductal adenocarcinoma. *Nat Genet*. 2023. doi:10.1038/s41588-023-01568-8

51. Sharma A, Seow JJW, Dutertre CA, et al. Onco-fetal Reprogramming of Endothelial Cells Drives Immunosuppressive Macrophages in Hepatocellular Carcinoma. *Cell*. 2020;183:377–394e21. doi:10.1016/j.cell.2020.08.040

52. Wang X, Wang J, Lyu L, Gao X, Cai Y, Tang B. Oncogenic role and potential regulatory mechanism of topoisomerase IIalpha in a pan-cancer analysis. *Sci Rep*. 2022;12:11161. doi:10.1038/s41598-022-15205-7

53. Chen M, Wei L, Law CT, et al. RNA N6-methyladenosine methyltransferase-like 3 promotes liver cancer progression through YTHDF2-dependent posttranscriptional silencing of SOCS2. *Hepatology*. 2018;67:2254–2270. doi:10.1002/hep.29683

54. Xia A, Yuan W, Wang Q, et al. The cancer-testis lncRNA lnc-CTHCC promotes hepatocellular carcinogenesis by binding hnRNP K and activating YAP1 transcription. *Nat Cancer*. 2022;3:203–218. doi:10.1038/s43018-021-00315-4

55. Brown JA, Kinzig CG, DeGregorio SJ, Steitz JA. Methyltransferase-like protein 16 binds the 3'-terminal triple helix of MALAT1 long noncoding RNA. *Proc Natl Acad Sci U S A*. 2016;113:14013–14018. doi:10.1073/pnas.1614759113

56. Su R, Dong L, Li Y, et al. METTL16 exerts an m(6)A-independent function to facilitate translation and tumorigenesis. *Nat Cell Biol*. 2022;24:205–216. doi:10.1038/s41556-021-00835-2

57. Sun Z, Hong Q, Liu Y, et al. Oviduct Transcriptomic Reveals the Regulation of mRNAs and lncRNAs Related to Goat Prolificacy in the Luteal Phase. *Animals*. 2022;12. doi:10.3390/ani12202823

58. Li H, Zhao J, Deng H, et al. N6-methyladenosine modification of PLOD2 causes spermatocyte damage in rats with varicocele. *Cell Mol Biol Lett*. 2023;28:72. doi:10.1186/s11658-023-00475-4

59. Wei H, Huang L, Lu Q, et al. N(6)-Methyladenosine-Modified LEAWBIH Drives Hepatocellular Carcinoma Progression through Epigenetically Activating Wnt/beta-Catenin Signaling. *J Hepatocell Carcinoma*. 2023;10:1991–2007. doi:10.2147/JHC.S433070

60. Tan C, Huang Y, Huang Z, et al. N(6)-Methyladenosine-Modified ATP8B1-AS1 Exerts Oncogenic Roles in Hepatocellular Carcinoma via Epigenetically Activating MYC. *J Hepatocell Carcinoma*. 2023;10:1479–1495. doi:10.2147/JHC.S415318